A thesis on

ENTRANCE CHANNEL EFFECT IN ^{82}Sr* USING DYNAMIC CLUSTER DECAY MODEL

Thesis submitted in partial fulfillment of the requirement for
The award of the degree of
Masters of Science
In
PHYSICS

Under
the supervision of
Dr. Manoj K Sharma

Submitted by
Ramneek Kaur
Roll no.- 30704013

School of physics and Material Science
Thapar UniversityPatiala – 147004 (PUNJAB) INDIA

CERTIFICATE

This is to certify that Ms. Ramneeek Kaur, Roll No. 30704013 has worked on this thesis report as a partial fulfillment for award of the degree of MASTERS OF SCIENCE in physics. I certify that the matter embodied in this report is of candidate's own record and not submitted to any other university in any part or full form for the award of such a degree.

9/7/09

(Dr. Manoj K Sharma)

Supervisor

SPMS, Thapar University

Patiala

Countersigned by:

10/7/09

Dr. O.P. Pandey

(Prof. & Head)

School of Physics and Materials Science

Thapar University, Patiala.

13/7/09

Dr. R.K. Sharma

Dean of academic Affairs

Thapar University

Patiala.

Acknowledgement

I owe my deepest gratitude to **Dr. Manoj K Sharma**, *my worthy supervisor*, who has been an inspiration during my research work. Without him, this dissertation would not have been possible. I thank him for his patience and encouragement that carried me on through difficult times, and for his insights and suggestions that helped to shape my research skills. I express my sincere thanks to him for his valuable guidance in carrying out work under his effective supervision, encouragement and cooperation. His visionary thoughts have influenced me greatly. His dynamical attitude has empowered me with zeal of energy to conquer the minor details of my research work.

I also thank **Dr. O. P. Pandey**, Professor and Head, School of Physics and Material Science for his support and providing facilities.

A special word of thanks to **Mrs. Shefali Kanwar**, Research Scholar for the help and valuable suggestions whenever I needed out of her busy schedule.

Special thanks to all my friends and the staff at the School of Physics and Material Sciences for providing me a friendly atmosphere and encouraging me throughout this work. Their assistance and partnership were of great pleasure. I am deeply thankful to my Family and my friend Gurpreet Kaur Bhullar, for their moral support and patience has bared fruit through completion of this Thesis

Ramneek Kaur

Ramneek Kaur

Roll no. 30704013

Date: July 9, 2009.

ABSTRACT

In view of present day developments in the domain of nuclear physics, it is extremely important & essential to study the nuclear properties and related phenomena at the extreme conditions of temperature, angular momentum & energies in order to respond the exotic experimentations being conducted & planned in near future. In order to meet such challenges, it becomes extremely essential to update the standard of theoretical computations in order to make meaningful predictions in the related field. In the last six decades since the discovery of nuclear fission, extensive theoretical and experimental investigations have been carried out to understand the various aspects of fusion-fission dynamics. One of the important feature in the domain of fission fusion in the concept & importance of entrance channel effects. It is therefore important to account for the entrance channel properties of target and projectile in order to study the fusion-fission dynamics.

Keeping this in mind, I have investigated the entrance channel effects in decay of $^{82}Sr^*$ formed in $^{16}O+^{66}Zn$ (Asymmetric) and $^{37}Cl+^{45}Sc$ (Symmetric) reactions. It is well established fact that the parameters which result in entrance channel effects are the barrier distribution, angular momentum anisotropies, mass asymmetry and nuclear deformations. The barrier distribution is due to presence of range of nuclear potentials across barrier and vibrations associated with projectile and target nucleus. Variation in angular momentum distribution results in different fission products. The deformations present in nuclear shapes results in different cross sections for interacting nucleus of target and projectile. Mass asymmetry factor also result in different type of fission fragments on decay of compound nucleus.

For the present study, I have used Dynamical Cluster Decay Model (DCM), which is a very vibrant model to account for nuclear fission dynamics in general & nuclear structure in particular. Our calculations clearly indicate that the entrance channel effect is extremely important parameter in deciding fission dynamic of a compound nucleus.

CONTENTS

CHAPTER 1

CHAPTER 2

LIST OF FIGURES

CHAPTER 1

CHAPTER 2

CHAPTER 3

LIST OF TABLES

CHAPTER 1

INTRODUCTION

Entrance channel effect in nuclear fission means decay of compound nucleus could be dependent or independent of it's mode of formation. There are numerous factors associated with interacting projectile and target on which formation and fission of compound nucleus depend. The statement that 'compound nucleus forgets its history of formation' gets violated for some observed reaction mostly in heavy mass region. The parameters which result in entrance channel effect are barrier distribution, angular momentum anisotropies, mass asymmetry and nuclear deformations. Barrier distribution is due to presence of range of nuclear potentials across barrier and vibrations associated with projectile and target nucleus. Variation in angular momentum distribution results in different fission products. Deformations present in nuclear shapes results in different cross sections for interacting nucleus of target and projectile. Mass asymmetry factor also result in different type of fission fragments on decay of compound nucleus.

All parameters which result in entrance channel effect can be studied by using dynamical cluster decay model (DCM) beside many statistical and non statistical models. The Entrance Channel effects are observed to be more common for heavy nuclear system because barrier distribution angular anisotropy, mass asymmetry, deformation and orientation of nuclear systems plays prominent role.

1.1 Recent Studies in Fusion-Fission Reactions

Nuclear fission in which nucleus divides into two fragments is one of the most interesting processes involving large scale collective nuclear motion. In the last six decades since the discovery of nuclear fission, extensive theoretical and experimental investigations have been carried out to understand the various aspects of this process. With the availability of the heavy ion accelerators in the sixties, there was added impetus in the study of dynamic of large shape changes

in nuclear system through the investigation of the nucleus-nucleus collision involving fusion of two nuclei followed by the fission process. This study in nuclear physics is termed as nuclear macrophysics; encompass various aspects dealing with the static mechanism of the nuclear system. Fusion-fission path are generally governed by the potential energy, impact parameter and the bombarding energy above the coulomb barrier. The dynamical evolution of a nuclear many body system can be described in terms of suitable collective coordinates which are coupled to intrinsic degrees of freedom by means of dissipative process. In light of the various investigations since early eighties, it is now well established fact that there is large scale damping of collective modes in heavy ion induced fission reactions, which result in large dynamical evolution in the decay process of nuclear system. Study of onset of the nuclear damping, signaling the transition from order to chaos in nuclear system is very important in order to understand the behavior of many body systems.

In the recent years, there have been many experimental observations which suggest possible occurrence of non-equilibrium modes of fission such as quasi fission, fast fission and a new mode called pre-equilibrium fission corresponding to partial equilibration of certain degrees of freedom during the heavy ion induced fission process. It is seen that these non-equilibrium processes occur in the heavy fissile system at all energies including sub barrier and near barrier. These non-equilibrium fission modes arises from the characteristics features of the potential landscapes in the multidimensional surface corresponding to the coordinate of deformation, mass asymmetry and neck degree of freedom and the dynamics underlying the large scale collective motion during the fission process. [1]

1.2 Compound Nucleus and Non-Compound Nucleus Formation

The fission of an atomic nucleus is a unique process in which a nuclear collective motion sets involving all nucleons in the nucleus and a large number of nucleons are eventually transported across the fission barrier. The possible decay modes of a compound nucleus are depicted in fig.1.1. A nucleus splits into two fragments during fission process and exhibit variety of shapes while transporting from equilibrium configuration to that of scission configuration. The instant at which the elongated heavy nucleus breaks into separate piece is called the scission point, and the two heavy pieces of nuclear matter formed instantaneously at scission are called primary fragments. The primary fragments sometimes called pre neutron figments (Hoffman and Hoffman 1974),[2] are usually at high excitation energy and cool down predominantly by neutron evaporation followed by γ-ray emission.

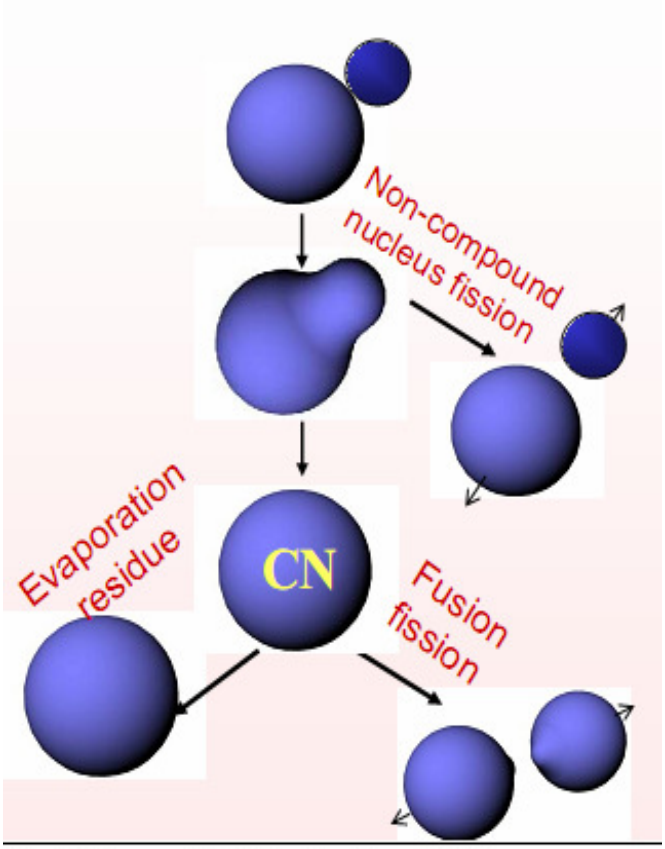

Fig.1.1 Decay of CN into ER, FF and NCN process

Fragments which no longer emit neutrons and finally de-excites by γ -ray emission are called secondary fragments. Unstable secondary fragments decay by p-emission until a stable nucleus formation take place. Fission cross sections of highly excited compound nuclei and pre-scission multiplicities of neutrons, light charged particles, and GDR γ- rays have been measured in the past to investigate the dynamics of fission. It is now established from all these studies that the measured values of pre-scission multiplicities of light particles and γ-rays are can

be measured with fare degree of accuracy. In general, it is almost established that contribution of fission fragments in light mass region is negligible in comparison to ER contribution whereas the trend is almost reverse in heavy mass region where fission process become a prominent decay channel. The enhancement in the number of the pre-scission neutrons (and other light particles and γ rays) immediately points to a slowing down of the fission process compared to the statistical model fission rate as given by Bohr Dynamical models. In other words there is a healthy competition between the ER, FF and QF process throughout the periodic table. During last two decades experimentalists have been seen immensely interested to investigate nuclear reaction dynamics at the extreme condition of temperature, angular momentum, deformations and orientations etc. The main purpose is to investigate the unexplored features of nuclear properties in general and nuclear forces in particular. As a consequence of this, it become almost essential to study the decay process of highly excited nuclear system formed in heavy ion reaction in order to meet the experimental observation and to make future predications.

In a dynamical model, the fission process is viewed as that of a Brownian particle in a viscous fluid. The degree of enhancement of pre-scission neutron multiplicity therefore depends on the strength of nuclear viscosity or the dissipative property of the nuclear bulk.

The pre-scission neutrons can be emitted at different stages of the fusion fission process. If fission is considered as a quasi stationary diffusion process over the fission barrier, a transient time is required for the system to build up a quasi stationary probability flow over the barrier. During this transition time, the fission process is inhibited though neutrons can be emitted. Thus the neutrons emitted during the transient time partially account for the enhancement of pre-scission multiplicity of neutrons. Thus more neutrons can be emitted in the dynamical model of fission than as predicted by the statistical model. This description however applies until the compound nucleus (CN) crosses the saddle point (saddle point is a point where nuclear system is about to explode). Beyond the saddle point, neutron evaporation from the CN can still continue till it reaches the

scission point. These saddle-to-scission neutrons make an additional contribution to the pre-scission neutron enhancement. These different stages of neutron emission however become effective only after a fully equilibrated CN is formed. [2,3,4]. In heavy-ion induced fusion reactions, the di-nuclear system that is formed in the entrance channel subsequently involves toward the compound nuclear system. The time scale of energy equilibration in the di-nuclear system is known to be much faster than the time scale of full equilibration. It is therefore possible that the energetically equilibrated di-nuclear system can emit neutrons before the fully equilibrated CN is formed. Thus the neutrons emitted during the CN formation time also contribute to the number of pre-scission neutrons. It is evident that the multiplicity of the formation-time neutrons depends on the entrance channel dynamics of the projectile-target system. Another competing process is a compound nucleus evolution is Quasi fission, where fragments keep their identity intact and hence the product remains same/similar to the reactants of the reaction.

1.3 Entrance Channel Effect

It is almost established that in addition to normal fission a fraction of fission events arises from a new reaction channel known as Preequilibrium fission events.

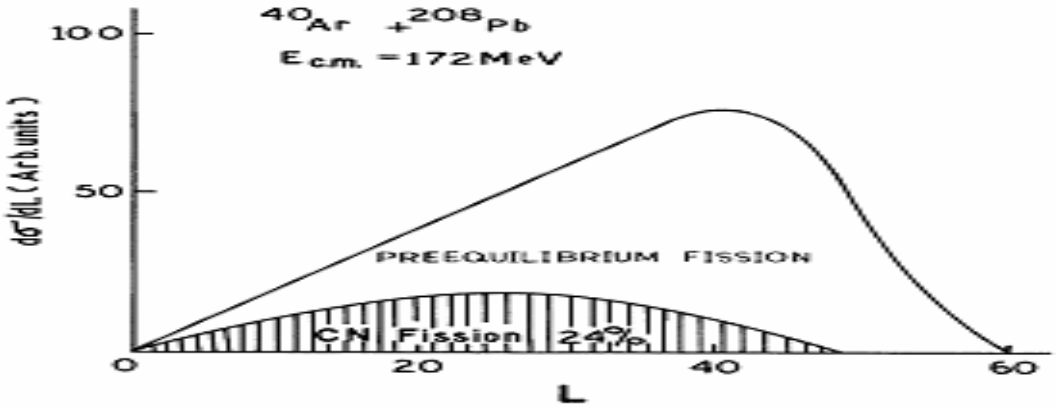

Fig.1.2 Differential cross-section as a function of angular momentum [L]

In case of Preequilibrium fused composite system become more compact than the fission saddle point, and fragments separated by the thermal diffusion over the barrier heights.

The collective degree which has lethargic relaxation in relation to compound nucleus equilibrium time is responsible for tilting of entrance channel reaction plane characterized by K-quantum number (explain K-quantum number). A memory of entrance channel plane will result in large fragment anisotropies measured in a number of heavy-ion-induced fission reactions. Therefore Preequilibrium contribution can be estimated from a study of the fragments anisotropies. The entrance channel mass/charge asymmetry in a heavy ion fusion reaction is continuously varied in order to investigate qualitative change in a fusion path. Compound nucleus formation is in general viewed from a critical symmetry criteria, as shown by the Businaro–Gallons critical asymmetry analysis which indicate that system having symmetries less than critical symmetry show deviation from the predication of standard statistical theory of fission fragment angular distributions. Boron, carbon, oxygen and fluorine induced fission of thorium have indeed revealed such a discontinuity in the entrance channel. Direct evidence for lethergetic relaxation of the tilting mode in heavy ion reaction has also come from the measurement of angular distribution for charge–separated fission like fragments.

Preequilibrium fission as described above is the additional limitation to compound nucleus formation over and above dynamical limitation if any, to reach the unconditional saddle point .Since the pre equilibrium fission fragment has also have large anisotropy ,as that for quasi fission events, so the differential fission cross section do not unambiguously identify fraction of fission following compound nucleus formation quasi fission and pre equilibrium fission. Therefore all attempts to deduce compound nucleus cross section from differential fission cross section without considering account of pre equilibrium contribution in general lead to misinterpretations. Such discrepancies are however, compensated to some extent in form of extra push energies. The fig 1.2 above shows collected cross section

for compound nucleus for different partial waves in $^{90}Ar+^{208}Pb$ reaction at E_{cm} =172Mev[11].

Preequilibrium fission take place after the passage over unconditional fission saddle point, a reduced equilibrium fission fraction does not signal a dynamical limitation to reach the saddle point. A detailed analysis of fragment angular distribution data in heavy ion induced fission reactions, is in progress to see whether the inclusion of preequilibrium fission, results in same compound nucleus as deduced from evaporation residue measurements or not.

1.4 Unexpected Entrance Channel Effect in Fission Process

In heavy/super heavy nuclear systems, prediction of absolute cross sections without extrapolation from nearby experimental cross sections is very challenging. This is due to extreme complexity of the process, and the very low probability of evaporation residue (ER) cross-section. The probability distribution of reaction outcome is extremely sensible to slight change in reaction condition and there exist healthy competition among quasi-fission and fusion-fission processes. Because of the very low yields of heavy elements, it is difficult and time-consuming to make detailed and systematic experimental studies for the reactions. However, such studies for reactions forming less fissile nuclei are more feasible, and can give valuable information on the dynamical processes occurring during the fusion of two nuclei. This information on dynamical process will also be relevant to reactions forming super-heavy elements.

The fusion–fission cross-section can conceptually be divided into three parts. In reality the three parts are not independent of each other, but are still sufficiently distinct to constitute a useful framework for discussion. These three points are discussed below:

The cross section for contact of the two colliding nuclei must be determined. Contact may be defined as a configuration where complex nuclear reactions between the two nuclei become highly probable. [5]

(A) For light systems, cross section is at a radius inside the peak in the potential barrier (capture barrier, or fusion barrier), and automatically leads to a compact compound nucleus.

(B) For collisions of heavier nuclei, cross section must be multiplied by the probability (less than unity) of reaching a compact shape inside the unconditional fission barrier. Collisions of heavier nuclei which do not achieve this compact shape contribute to the quasi-fission or deep-inelastic yield. For composite nuclei achieving a compact shape, the yield of the evaporation residues is determined by the probability of surviving fission decay from this compact configuration. The identity of the nuclei reaching the compact shape will be dependent on particle evaporation during the dynamical phase. Thus the evaporation residue (ER) formation cross section may be written:

$$\sigma_{ER}(E^*, \ell) = \sigma_{contact}(E^*, \ell, EC) \cdot P_{compact}(E^*, \ell, EC) \cdot P_{surv}(E^*, \ell) \qquad (1)$$

Where $\sigma_{contact}(E^*, \ell, EC)$ is the cross section for capture, for excitation energy E^* of the heavy nucleus with angular momentum $\ell\hbar$, and in general depends on specific entrance channel (EC)conditions. $P_{compact}(E^*, \ell, EC)$ is probability of passing to a compact shape.[7,8]

$$P_{surv}(E^*, \ell) = [1 - P_{fis}(E^*, \ell)]$$

The survival probability against fission from the compact shape. It is re-emphasized that in reality, the nucleus will cool by evaporation during the transition to the compact shape, so the latter two factors are not independent. $P_{compact}(E^*, \ell, EC)$ is complementary to the probability of quasi fission $P_{QF}(E^*, L, EC)$, namely $P_{compact} + P_{QF} = 1$. To maximize the heavy nucleus survival cross section, the product of all three factors must be maximized. As in heavy element synthesis, the physical processes associated with the entrance channel can make it impossible to simultaneously maximize all three factors individually. So, when we include effect of entrance channel cross section for evaporation residue will $P_{compact}$ will not have its maximum value. The $P_{compact} + P_{QF} = 1$ [7,6]can be written as $P_{QF} = 1 - P_{compact}$. There will be more chances of decay by quasi

fission which clearly mean that presence of quasi fission result in hindrance of evaporation residue.

1.5 Role of the Entrance Channel Dynamics on the Evaporation Residue Formation

The comparison of the capture and fusion cross sections of nuclear reactions leading to the same compound nucleus shows a dependence of the reaction mechanism on the shell structure and mass asymmetry of the projectile-target pair. This allows us to determinate favorable conditions for the synthesis of super heavy elements, production of nuclides far from the region of stability in heavy ion collisions. The capture of the projectile by the target is calculated as a trap of the system into pocket of the nucleus-nucleus potential after dissipation of the kinetic energy and orbital angular momentum of the relative motion. Friction and mass coefficients are found by calculation of the evolution of the coupling term between the relative motion of nuclei and the intrinsic excitation of nucleons and nucleon exchange in Di-nuclear system DNS [9]. The complete fusion being considered as the transformation of the di nuclear system into compound nucleus is calculated statistically. The dependence of the excitation function of evaporation residues on the mass asymmetry of the colliding nuclei is connected with the formation of the same compound nucleus with different angular momentum distribution. One may that the yield of evaporation residues in the mass asymmetric reactions is significantly larger in comparison with the more symmetric reactions due to the smallness of the intrinsic fusion barrier and larger quasi fission barrier.

Measurements of evaporation residues cross section for reactions leading to the same compound nuclei can be explained by the difference in the excitation functions of capture and fusion, as well as by the difference in survival probabilities of the excited compound nucleus. The models based on the dinuclear system concept (DNS) can be used to reveal reasons causing the strong decrease in the fusion cross section for a massive system or for a more mass symmetric reactions. The decrease of fusion probability, in these cases,

occurs due to increasing of contribution of quasi fission process. Calculations based on the DNS concept showed [9,10] that the peculiarities of the entrance channel are important to describe or interpret the experimental data obtained in reactions of massive nuclei. The study of the role of entrance channel in formation of evaporation residue products reveals that the angular momentum distribution of compound nucleus is defined by dynamics of capture and fusion stages of reaction. Both the experimental and theoretical studies are needed to be are elevated to account for optimal conditions for the synthesis of new super heavy elements. The effect of the entrance channel peculiarities in formation of evaporation residues is recognized by the partial capture and fusion cross sections studies

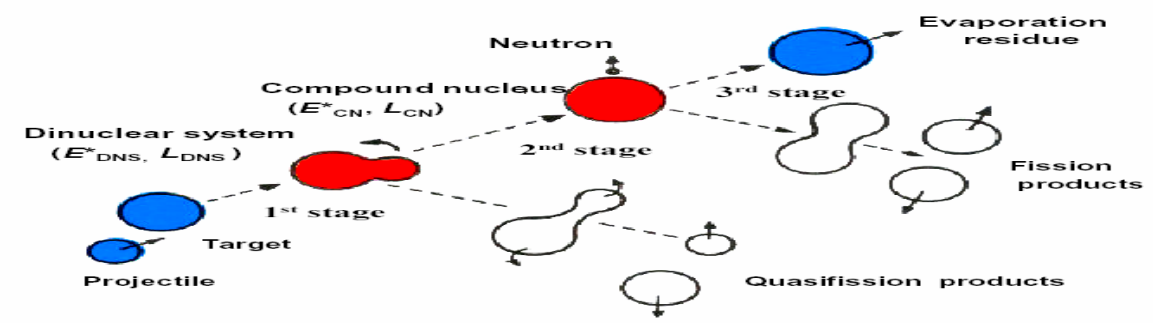

Fig.1.3 Description of Formation and decay of the nuclear system

1.6 Parameters which Results in Entrance Channel Effect are:

1.6.1 Entrance Channel Barrier Distribution

1.6.2 Entrance Channel Mass Asymmetry

1.6.3 Angular Distribution of Fission Fragments

1.6.4 Deformations in Nuclear Shapes

1.6.1 Entrance Channel Barrier Distribution

It is well-established that in collisions of heavy nuclei, there is not a single potential barrier, but a distribution of barrier energies, where D(E) is defined as

the probability of encountering a barrier of energy E, and can be determined directly from experimental capture cross sections closely-spaced in energy .The barrier distribution depend on following factors of interacting nuclei

(a)The distribution can be understood classically in the case of statically deformed nuclei, where different orientations of the deformation axis with respect to the incident projectile result in potential barriers at different radii, this result in energy difference for different orientation of target and projectile.

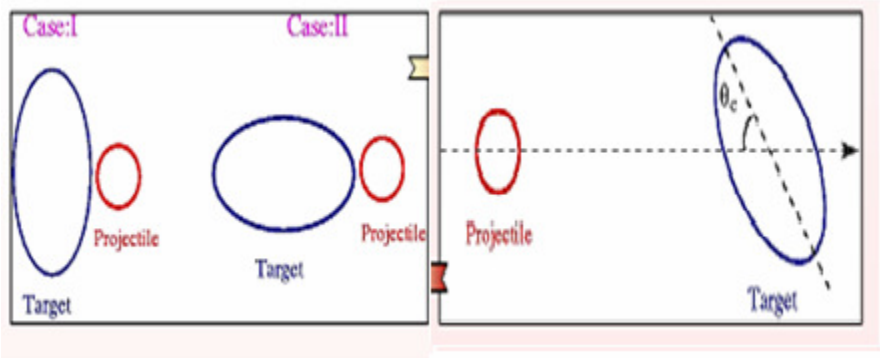

Fig 1.4 Interaction of target and projectile at entrance channel

Two different cases for the injection of the projectile at the tip and flattened side of the target. It is relevant to mention here that head on collision [3]

Case: I Result in relatively large cross section than side collision

Case: II The fusion hindrance in side collision can be overcome via well known extra push energies.

Case: III The fusion of the projectile colliding on the surface of the deformed target up to a critical angle generates QF. The orientated distribution of projectile target combination in general result in barrier distribution .Barrier distribution become shallow and as a result fusion probability gets enhanced by significant amount.

Strongly-coupled collective vibrations and multi-nucleon transfer can also give rise to broad barrier distributions. The concept of the barrier distribution can be extended by the cases where the intrinsic motion of interacting nuclei carries a finite excitation energy Coupled-channels calculations have shown that the fusion barrier distribution, i.e. $d^2(E\sigma)/dE^2$, is very sensitive to the details of the channel couplings, To observe their sensitivity to the couplings, the excitation function of

fusion cross sections has to be measured with high precision at small energy intervals. Recently experiments has shown that the barrier distribution is indeed a sensitive quantity to the channel couplings [8].It show the effects of couplings due to static deformations and associated rotational motions, vibrational degrees of freedom, and transfer reactions, in a way much more apparent than in the fusion excitation function itself. These high precision data have, thus enabled a detailed study of the effects of nuclear collective excitations on fusion reactions, and have generated a renewed interest in heavy-ion sub barrier fusion reactions [8].

Typically, the width of the barrier distribution is between 5% to 10% of the mean barrier energy. Although these different barriers effect all reaction processes, if we particularly have capturing of (or fusion, for lighter systems). In general for light nuclear system quasi-fission is not present the entire mass inside the potential barrier lead to an equilibrated compound nucleus. It is possible to identify the sum of the fission and evaporation residue yields with passage inside the capture barriers, and the term fusion barrier distribution is appropriate in this regime. For heavier systems, though the two nuclei may be captured inside the potential barrier, they are likely to re-separate after energy damping and mass-exchange (deep inelastic or quasi- fission processes).

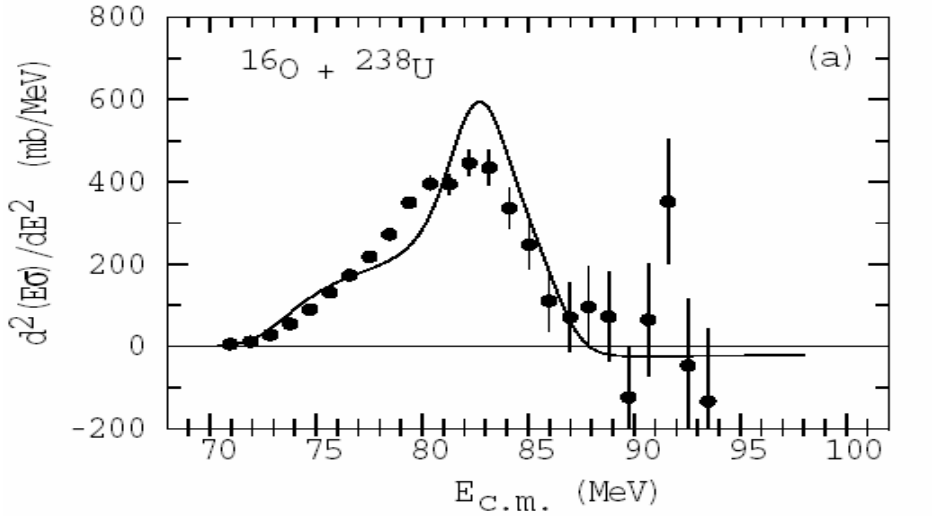

Fig1.5 Decay before equilibrium of compound nucleus. The capture barrier distribution for $^{16}O+^{238}U$

In heavy/ super heavy nuclei formation, the entrance-channel model describes the capture cross sections, and so we refer to the capture barrier distribution. It is important to note here that the capture cross section is only one of the factors which effect the ER cross section. Therefore it becomes extremely essential to have systematic study of entrance channel effects in order to calculate barrier probability for a compact nucleus formation. The capture barrier probability distribution for $^{16}O + ^{238}U$rection is as shown in Fig.1.5. The presences of the wide capture barrier distributions which necessarily occur during the collision of two heavy nuclei constitute a significant element in interpretations or predictions of cross sections for reactions forming heavy/super-heavy nuclei. In general, reactions at energies below the uncoupled potential barrier occur not through tunneling through that barrier, but by passage over a lower barrier, which is encountered with a probability defined by the barrier distribution. In the language of Myers and Swiatecki those collisions which actually lead to very heavy nuclei are almost certainly “unshielded”, the capture barrier having been below the bombarding energy. The fact that there is almost no potential pocket for the uncoupled barrier will surely influence the extent and probability of finding barriers at energies lower than the uncoupled barrier. To maximize ER cross sections, not only the weights (probabilities) of these lower barriers be maximal, but the elongation of the composite nucleus at contact, after passing the potential barrier, should also be as small as possible.

1.6.2 The Entrance Channel Effect Due To Mass Asymmetry

We take mass of target A_t and mass of projectile as A_p then we write α as:

$$\alpha = (A_t - Ap)/(A_t + A_p).$$

It is further known that the fusion paths followed by two composite systems with $\alpha<\alpha_{BG}$ and $\alpha> \alpha_{BG}$, where α_{BG} is the critical Businaro-Gallone mass asymmetry are quite different are chosen to form the same CN. Though a substantial amount of work has been done in the past on the measurement of multiplicity of pre-scission neutrons, the number of experimental investigations focusing on the role

of entrance channel mass asymmetry in pre-scission neutron multiplicity is rather limited.[7,8]

The pre-scission neutron multiplicity by populating ^{248}Cf through two different entrance channels lying on either side of the critical Businaro-Gallone mass asymmetry and found more pre-scission neutrons from the system $^{16}O + ^{232}Th$ ($\alpha<\alpha_{BG}$) than from $^{11}B + ^{237}Np$ ($\alpha>\alpha_{BG}$).In the resent work, we have measured the pre-scission neutron multiplicity from $^{16}O + ^{181}Ta$ ($\alpha = 0.837$) and $^{19}F + ^{178}Hf$ ($\alpha = 0.807$) reactions lying on the two sides of the Businaro-Gallone point ($\alpha_{BG} = 0.814$). The measurements are made at different laboratory energies, which are chosen such that the ^{197}Tl compound nucleus is formed at the same excitation energies in the two reactions. [7,8,11]

The dynamical calculations show that the formation time for the compound nucleus for the symmetric system is relatively larger as compared to the asymmetric system.However,dynamicals effects leads to formation of temperature equilibrated intermediate di-nuclear complex, this temperature balancing is due to emission of high energy neutrons.

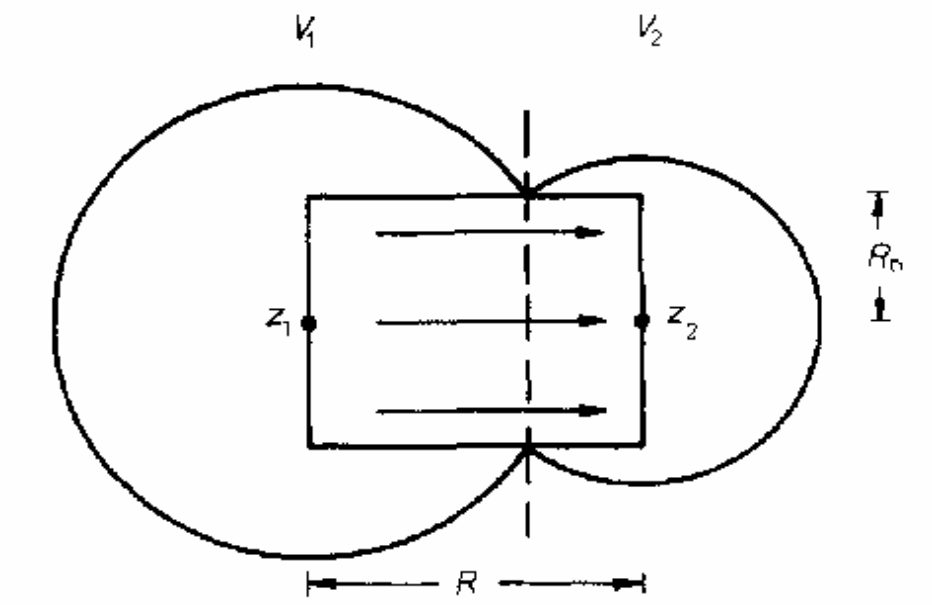

Fig1.6 Mass transfer in collision

During collision of target and projectile there is transfer of mass between them to form a compound nucleus. This can be explained with the help of classical model for the mass tensor of the kinetic energy in heavy-ion collisions. The model is based on the hydro dynamical flow picture and allows one to calculate analytic expressions for the masses of the relative motion and transfer of mass.

In the simplest representation this model can be treated as follows .The two nuclei are assumed to be spheres if they are separated, and connected semi sphere if they have overlapped their shape is shown in figure1.6.

The relative distance $R = z_1 - z_2$, between the centres at z_1 and z_2 and the mass asymmetry coordinate $\eta = (V_1 - V_2)/V$, where V is the total conserved volume and V_l and V_2 the volumes on the left and right sides of the plane through the neck. For the mass flow we assume a homogeneous flow in the volume V_l with velocity Z'_1, in V_2 with Z'_2, and in V_o with V_T**.** The volume V_o is the cylindrical inner region bounded by the centres of the semi spheres and the neck with radius R. The velocities are referred to a system where the plane through the neck is fixed. Then the transfer velocity $\dot{\eta}$ is related to V_T

$$V_T = (RV/2V_o)\,\dot{\eta}$$

The kinetic energy results after subtraction of the centre-of-mass **(CM)** energy as

$$T = 1/2B_{RR}\,\dot{R}^2 + B_{R\eta}\dot{R}\dot{\eta} + 1/2B_{\eta\eta}\,\dot{\eta}^2$$

$$B_{RR} = 1/4M(1-\eta^2)$$

$$B_{\eta\eta} = M/4R^2\,(V/V_0-1)$$

Here M is the total mass and $V_o = \pi RR^2{}_n$.

The mixed mass $B_{R\eta}$ is small $(B_{R\eta} < (B_{R\eta}\,B_{RR})^{1/2})$.

This model is simple enough to give comprehensive expressions for the transfer mass, but it is also realistic enough to yield qualitative agreement with hydro dynamical and microscopic calculations.

1.6.3 Entrance Channel Effect in Fission Fragment Angular Distribution

An approximate expression[4] for fission anisotropy is given by

$$A = (1+ <\ell^2>) /4K^2,$$

where $<\ell^2>$ is the mean square angular momentum $K^2= (J_{eff}/h^2)T$ where J_{eff} is the effective moment of inertia at the saddle point and T is the saddle point temperature.

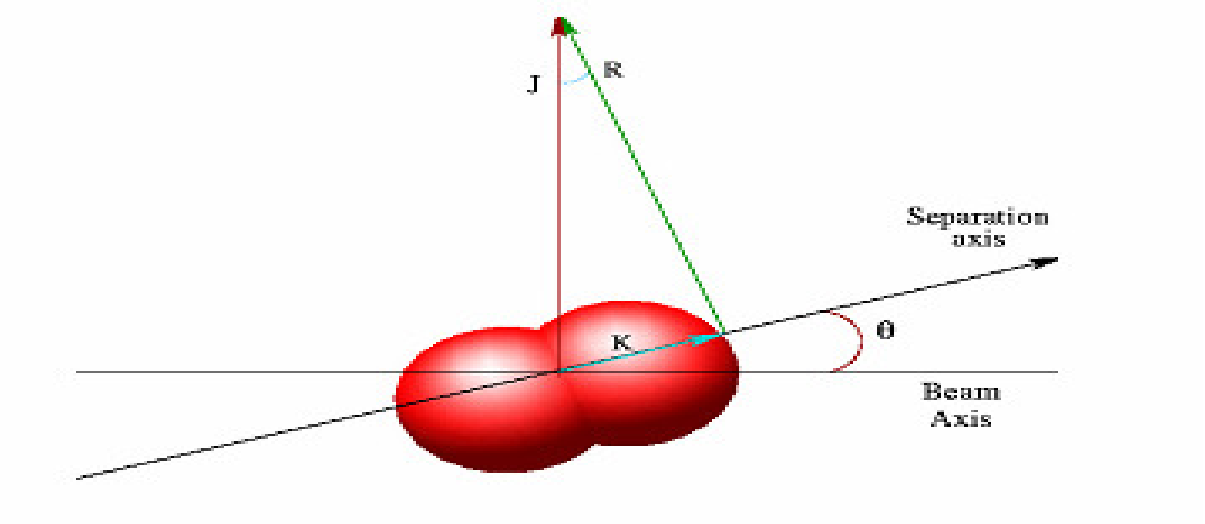

Fig. 1.7 Depending upon entrance channel Mass asymmetry the composite system may decay before K equilibrium

In Fig.1.7 the $<\ell^2>$ values determined from fitting the fusion/fission excitation functions are plotted as a function of the compound nucleus excitation energy values for the two different systems investigated. It can be seen from the Fig. I.7 [5,13,14]

It can be seen from the figure1.8 that at similar excitation energy values, the measured anisotropies for $^{14}N+^{232}Th$ case are larger than that for $^{11}B+^{235}U$. From Fig. I.8, it is observed that the corresponding $<\ell^2>$ values for $^{14}N+^{232}Th$ are always less than that for $^{11}B+ ^{235}U$ in the range of excitation energies plotted. The above result implies an entrance channel effect at these excitation energies.

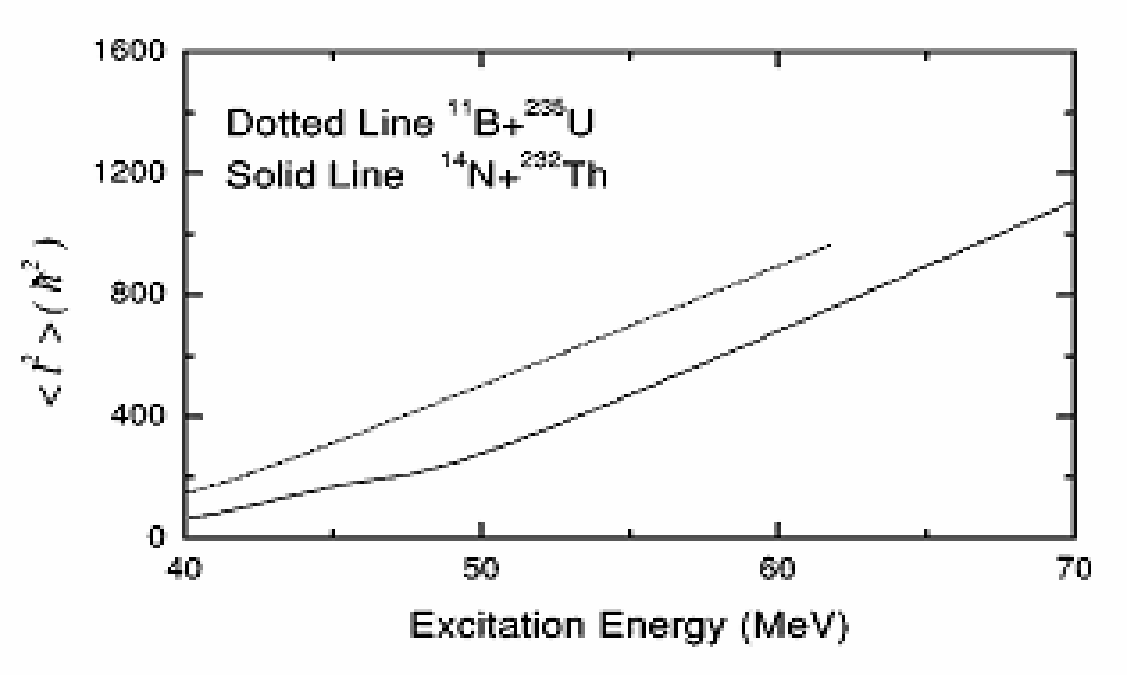

Fig.1.8 The mean square angular momentum $< \ell^2 >$ derived from fit to fission excitation function

One may expect $^{1}B+^{235}U$ system to show normal behavior with respect to SSPM. It is not known a priori whether $^{14}N + ^{232}Th$, will show normal or anomalous behavior. In both the cases anisotropies were calculated on the basis of SSPM.As mentioned above, the required spin distribution of the compound nucleus. Thus the results clearly indicate that between 40MeV and 60 MeV of excitation energy there is a possibility of entrance channel effect for $^{11}B + ^{235}U$ and $^{14}N + ^{232}Th$ channel.

1.6.4 Entrance Channel Effect and Deformation

In many respects spherical nuclei are exceptional, as the vast majority of nuclei are deformed. Many nuclei are only slightly non-spherical, and so can still be well described by spherical nuclear models. However, for nuclei with a mass number *A* in the range $150 < A < 200$ and $A > 220$ deformation can no longer be ignored. Most nuclei, however, tend to be deformed because their shells are only partially filled. The most commonly encountered shapes are elongated (prolate) or

flattened (oblate); these shapes can change from one nucleus to its neighbour by adding or removing a proton or neutron. In some cases it is sufficient to rearrange the protons or neutrons within the same nucleus to change its shape. The same nucleus can therefore assume different shapes corresponding to states of different energy. The entrance channel effects can emerge when we transport from two body shape to one body shape. A selected shape sequence is depicted in fig1.8 below. Mathematically, these quasi molecular shapes correspond to two joined elliptic lemniscatoid assuming volume conservation. Analytic formulae are avail-able for the main shape-dependent functions: volume, surface, distance between mass centers and moment of inertia. Similar compact shapes have been also adopted to determine the energy of super heavy nuclei. For the exit channel these shapes implicitly suppose that the particle is rather formed at the surface of the parent nucleus.[3,6]

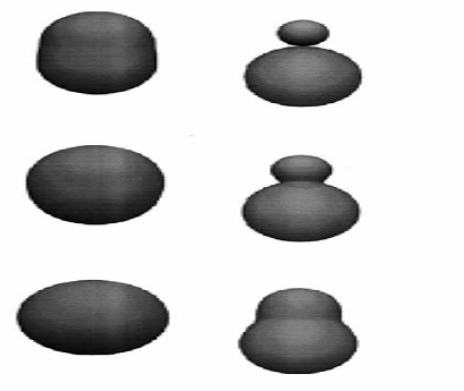

Fig1.9 Selected shape sequence to simulate the transition from two body to one body shapes and alpha decay path the nuclei are spherical

For moderately asymmetric reactions double-hump potential barriers stand and fast fission of compact shapes in the outer well is the main exit channel. Very asymmetric reactions lead to one hump barriers which can be passed only with an energy much higher than the ground state energy of the compound system. Then, only emission of several neutrons or an alpha particle can stabilize the nuclear system and allows reaching a ground state. The formation of heavy/super heavy elements via almost symmetric

reactions is a rare process. For heavy systems, with large coulomb repulsion, there is a dramatic reduction of the true fusion probability, which serves as a obstacle in formation of super heavy elements. Because of high probability of fission, obtaining detailed information about this effect is very hard task. We can study only those nuclei which survive fission. The classical way of studying collision results that higher barrier correspond to contact of the projectile with the flattened side of prolate target which initially result in a compact di-nuclear system .Conversely the lower barrier corresponds to contact with tip which is giving an elongated di-nuclear system.

Synthesis of a heavy element, which is made by heavy ion fusion reactions, is an important and exciting issue for nuclear physics. Because the decay properties of the heavy ion give information on the shell effects of nucleus, without which such a heavy nucleus could not exist due to overwhelming repulsive Coulomb force. It is generally accepted that the production of evaporation residues comprises of two separate processes, the fusion between two interacting nuclei (entrance channel) and the survival against fission in the course of the de-excitation process (exit channel). The former process is successfully described by a coupled channel model for projectile-target combinations with Z_1Z_2 ~ 1800. On the other hand, in heavy systems ($Z1Z2$ >1800), the formation of a compound nucleus is hindered. This is caused by the friction generated between the interacting two nuclei in the course of fusion process. The friction force decreases the kinetic energy of the nuclei, which hinders a complete fusion. To drive the system to the compound nucleus, an additional bombarding energy is needed above the Coulomb barrier to compensate for the energy loss by friction, which is called extra-extra-push energy (EXX).The extra push energy becomes more significant for heavier target projectile combination.

REFERENCES:

(1)R.K Choudhury and S.S Kapoor Nuclear Physics Division, Bhabha Atomic research Center Mumbai 400 085(India)(Received 29 October 1999;Accepted 29 May 2000)

(2) M. Satpathy, and S.K. Dattae Nuclear Physics A734 (2004) 249-252

(3) G. Royer, K. Zbiri, C. Bonilla 1Laboratoire Subatech, UMR: IN2 P3/CNRS-Universit´e-Ecole des Mines,4 rue A. Kastler, 44307 Nantes Cedex 03, France

(4) BirBikram Singh,1Manoj K. Sharma,1and Raj K. Gupta21School of Physics and Material Science, Thapar University, Patiala-147004, India 2Department of Physics, Panjab University, Chandigarh-160014, India (Received 24 March 2008; published 28 May 2008)

(5) G. Royer, K. Zbiri, C. Bonilla 1Laboratoire Subatech, UMR: IN2P3/CNRS-Universit´e-Ecole des Mines,4 rue A. Kastler, 44307 Nantes Cedex 03, France

(6) D. J. Hinde,A. C. Berriman, R. D. Butt, M. Dasgupta, I. I. Gontchar,C. R. Morton,A. Mukherjee, and J. O. NewtonJournal of Nuclear and Radiochemical Sciences,Vol. 3, No. 1, pp. 31–38, 2002

(7) J P Lestone, A A Sonzogni, M P Kelly and R Vandenbosch
Nuclear hysics Laboratory, University of Washington, Seattle, WA 98195,USA

(8) K. Hagino1, S. Kuyucak2, and N. Takigawa1Australian National University, Canberra, ACT 0200, Australia

(9) *Fazio G. et al.* Strong influence of the entrance channel on the formation of compound nuclei 216,222Th* and their evaporation residues // Phys. Rev. - 2005. - Vol. C72. - P. 064614 (14 pages).

(10) *Fazio G., Giardina G., Lamberto A. et al.* The infuence of the entrance channel dynamics on the evaporation residue formation // Eur. Phys. Jour. - 2004. - Vol. A22. - P. 75 - 87.

(11) Saha Institute of Nuclear Physics, Calcutta 700 064, India(huhg) Bivash R. Behera, S. Jena, and M. SatpathyDepartment of Physics, Utkal University, Bhubaneswar 751 004, India

(12) D. J. Hinde et al., Phys. Rev. Lett. 74, 1295 (1995)

(13) Ramammurthy and Kapoor, Phys. Rev. Lett. 54, 178 (1985)

(14) R. Vandenbosch, J. D. Bierman, J. P. Lestone, J. F. Liang, D. J.Prindle, A. A. Sonzogni, S. Kailas, D. M. Nadkarni, and S. S.Kapoor, Phys. Rev. C 54, R977 ~1996

CHAPTER 2

METHODOLOGY

2.1 Introduction

A comprehensive study of various types of emission from the ground state as well as excited states of compound nucleus (CN) formed in low energy reaction is important, as it gives information about the nuclear structure aside the underlying nuclear forces .At low energies and average nuclear force field acts between decaying fragments which in turns ensure possibility of more than one decay path. This average nuclear force field is largely influenced by entrance channel, angular momentum and the temperature consideration along with contribution of deformed and orientation effects. An extensive study of these nuclear properties lead to a better understanding of reaction dynamics of rare nuclear species that make the unexplored part of the nuclear chart, called exotic nuclei.

The main aim of the work is to study heavy ion reaction dynamics especially the decay of excited compound nucleus using the dynamical cluster decay model (DCM)[1]-[9]. It is important to note that deformation and orientation effects of the reaction partner and decay products are explicitly included along with temperature and angular momentum contribution in this model. The ground state cluster decay of radioactive nuclei has also been undertaken with in the preformed cluster decay model [10]-[18]. Again having deformation and orientation effects of the cluster as well as daughter nuclei included in it. Details of DCM and PCM are given in the section 2.2 and 2.6 respectively both of which stem from the Quantum Mechanical Fragmentation Theory, (QMFT)[19]-[32] which in binary fragmentation, uses a collective mass transfer process.

This model is a two step model, where the first step is quantum mechanical preformation probability P_0 of the decay products or cluster formed in the mother nuclei and the second step is the penetration of the fragments/ clusters through the interaction barrier. The P_0 based on QMFT is also discussed

here in section 2.3.7. The details for penetration probability P are given in section 2.4.These two crucial parameters (P_0 and P) have been developed and used [9], [17], [18], [33,] [34], to incorporate the deformation effects of oriented nuclei. The assault frequency, ν_0 with which the preformed cluster tries to tunnel the barrier in the ground state decay is discussed in section 2.5

2.2 The Dynamical Cluster Decay Model (DCM) For Hot and Rotating Compound Nucleus

The dynamical cluster decay model (DCM) [1]-[9] for hot and rotating nuclei (i.e. angular momentum and temperature both not equal to zero) is a reformation of the preformed cluster model of Gupta and collaborators for ground state decay (ℓ =0,t=0)in cluster radioactive (CR)and related phenomena [10]-[18] .Like PCM and DCM is also based upon the dynamical (or quantum mechanical) fragmentation theory of cold phenomena in heavy ion reaction and fission dynamics .In DCM, besides the temperature and angular momentum effects in the decay of excited compound nuclei ,the deformation and orientation effect of the decay products are also taken care, especially in the decay of heavy excited CN for which the deformation of the decay product seems to play significant role. The DCM, worked out in terms of the collective coordinates of mass asymmetry

$\eta=\frac{A_1-A_2}{A_1+A_2}$ and relative separation R respectively gives:

(i). The nucleon-division (or exchange)between the outgoing fragments.

(ii). The transfer of kinetic energy of incident channel (E_{cm}) to internal excitation (total excitation or total kinetic energy ,TXE or TKE) of the outgoing channel .It may be noted that the fixed decay point R = R_a (defined later),at which the process is calculated depends upon temperature T as well as on η (i.e.R(T, η)) .This energy transfer process can be calculated as follows with the help of Fig 2.1

E^*_{CN} = $E_{c.m} + Q_{in}$ = $IQ_{out}I + TKE(T) + TXE(T)$

The CN excitation E^*_{CN} is related to T (in MeV) and is given by

$E^*_{CN} = \frac{1}{9}AT^2 - T(Mev)$.

Using the decoupled approximation to R and η–motions, the DCM define the decay cross section ,in terms of partial waves, as[3]-[9] ;

$$k = \sqrt{\frac{(2\mu Ec.m)}{\hbar^2}}; \sigma = \sum_{l=0}^{lc} \sigma l = \frac{\pi}{k^2}\sum_{l=0}^{lc}(2l+1)PoP \qquad (2.2)$$

Where P_o ,the preformation probability refers to η-motion and P, the penetrability to the R- motion, discussed in section 2.3.7 and 2.4 respectively .Here the complex fragments (both light and heavy fragments) are treated as the dynamical collective mass motion of preformed cluster or fragments through the barrier .The structure information of the CN enters the model vai preformation probability P_o (also known as spectroscopic factor)of the fragments given by the solution of stationary Schrödinger equation in η at the fixed $R=R_a$, the first turning point of the penetrability path shown in figure 2.1for the different ℓ -values .

$$\left\{-\frac{\hbar^2}{2\sqrt{B_{\eta\eta}}}\frac{\partial}{\partial\eta}\frac{1}{\sqrt{B_{\eta\eta}}}\frac{\partial}{\partial\eta}+V_R(\eta,T)\right\}\psi^{\nu}(\eta)=E^{\nu}\psi^{\nu}(\eta) \qquad (2.3)$$

with ν =0,1,2,3,….referring to the ground state and excited state solution .

For the decay of the hot compound nucleus, we use the postulate of first turning point

$$R_a=R_t+\Delta R(T) \qquad (2.4)$$

Where

$$R_t = R_1+R_2 \qquad (2.5)$$

ΔR(T) is the neck length parameter that assimilates the neck formation effects .This method is introducing a neck length parameter similar to that used in scission point [35] and saddle point [36],[37]statistical fission model. The R_i are radius vectors which are also made temperature dependent can be calculated as

$$R_i(\alpha_i) = R_{0i}\left[1+\sum_{\lambda}\beta_{\lambda i}Y_{\lambda}^{(0)}(\alpha_i)\right] \qquad (2.6)$$

with

$$R_{0i}(T) = 1.28A_i^{1/3} - 0.76 + 0.8A_i^{-1/3} \times (1 + 0.0007T^2), \quad (2.7)$$

The corresponding potential V (R_a) acts like an effective Q-value, Q_{eff}, for the decay of the hot CN at temperature T, to two exit-channel fragments observed in g.s. (T=0), defined by

$$Q_{eff}(T) = B(T) - [B_L(T=0) + B_H(T=0)]$$
$$= TKE(T) = V(R_a(T)) \quad (2.8)$$

with B's as the respective binding energies.

The above defined decay of a hot CN into two cold (T=0) fragments, via Eq.(2.8), could apparently be achieved only by emitting some light particle (s)(LPs), like n, p, α, or γ-rays of energy.

By defining Q_{eff} (T) as in Eq. (2.8), in this model we treat the LP emission at par with the heavy fragments, called intermediate mass fragments (IMFs) emission. Thus, in this model a non-statistical dynamical treatment is attempted for not only the emission of IMFs but also of multiple LPs, understood so-far only as the statistically evaporated particles in a CN emission. It may be reminded here that the statistical model (CN emission) interpretation of IMFs is not as good as it is for the LP production [35 – 40].

In terms of Q_{eff} (T), the second turning R_b satisfies (see Fig. 2.1)

$$V(R_a, l) = V(R_b, l) = Q_{eff}(T, l) = TKE(T). \quad (2.9)$$

with the l-dependence of R_a defined by

$$V(Ra, l) = Q_{eff}(T, l = 0), \quad (2.10)$$

which means that the R_a, given by Eq. (2.4), is the same for all l -values, and that V (Ra, l) acts like an effective Q-value, Q_{eff} (T, l), given by the total kinetic energy TKE(T). Then, using (2.9), $R_b(l)$ is given by the l-dependent scattering potentials, at fixed Tas

$$V(R, T, l) = V_c(Z_i, \beta_{\lambda i}, \theta_i, T) + V_p(A_i, \beta_{\lambda i}, \theta_i, T)$$
$$+ V_l(R, A_i, \beta_{\lambda i}, \theta_i, T) \quad (2.11)$$

which is normalized to the exit channel binding energy $B_L(T) + B_H(T)$.

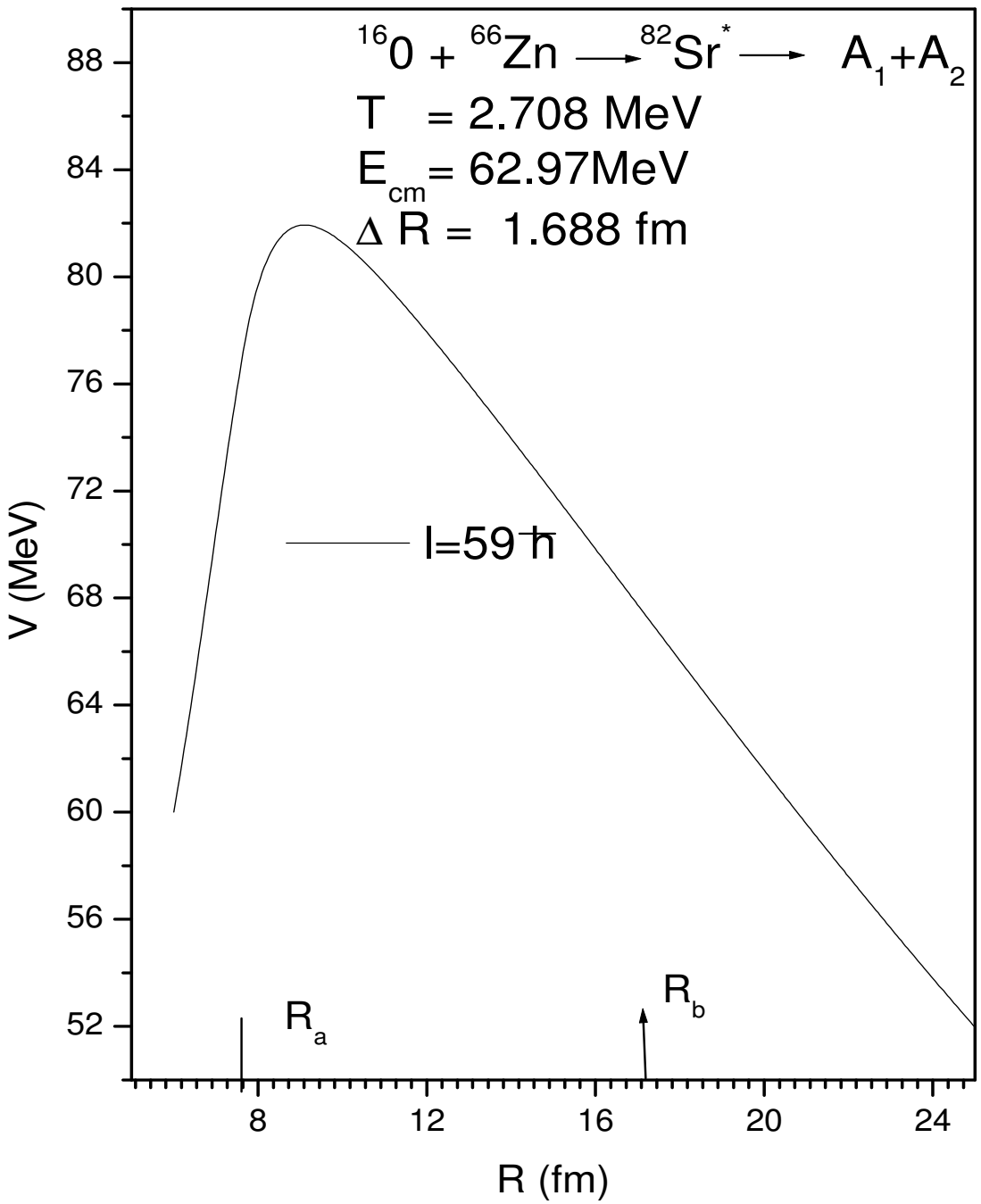
$^{16}0 + {}^{66}Zn \longrightarrow {}^{82}Sr^{*} \longrightarrow A_1+A_2$
T = 2.708 MeV
E_{cm} = 62.97MeV
Δ R = 1.688 fm
l=59ħ
R_a
R_b
V (MeV)
R (fm)
88
84
80
76
72
68
64
60
56
52
8
12
16
20
24

Fig2.1 Scattering Plot for $^{16}O+^{66}Zn \rightarrow {}^{82}Sr \rightarrow A_1 + A_2$ at $l = 59\ \hbar$

Such a potential is illustrated in Fig.2.1, $^{16}O+^{66}Zn \rightarrow {}^{82}Sr$, at different l -values. The second turning point R_b is marked for the l = 0ħ case of $R_a = R_t + \Delta R(T)$. Note that as the l -value increases, the Q_{eff} (T)-value (TKE(T)) increases and hence V (R_a, l) increases, since the decay path for all the l -values begins at R = R_a.

The collective fragmentation potential V (R, η, T) in Eq. (2.11) is calculated according to the Strutinsky method by using the T-dependent liquid drop model energy V_{LDM} of [41], with its constants at T=0 re-fitted [3, 4] to give the recent experimental binding energies given by [42], and again refitted [9] to give the recent experimental binding energies[43] and calculate binding energies[44] (only for those nuclides for which experimental data is not available. the "empirical" shell corrections δU are of Ref. [45] (In the Appendix of [3] and Eq. (8) of [4], a_a=0.5, instead of unity). Then, including the T-dependence also in Coulomb, nuclear proximity, and l -dependent potential in complete sticking limit of moment of interia , we get

$$V(R,\eta,T) = \sum_{i=1}^{2}[V_{LDM}(A_i,Z_i,T) + \sum_{i=1}^{2}[\delta Ui]exp\left(\frac{-T^2}{T_0^2}\right) + V_c(Z_i,\beta_{\lambda i},\theta_i,T) + V_P(A_i,\beta_{\lambda i},\theta_i,T) + V_l(R,\beta_{\lambda i},\theta_i,T) \quad (2.12)$$

where the T-dependent terms V_c, V_P and V_l are defined as follows: The proximity potential for hot deformed nuclei is [33],[34] (see section 2.3.3)

$$V_p(A_i, \beta_{\lambda i}, \theta i, T) = 4\pi\bar{R}\,(T)\gamma b(T)\Phi(s_0(T)) \quad (2.13)$$

and, the Coulomb Potential (see section 2.3.4)

(2.16)

$$V_c\left(Z_i, \beta_{\lambda i}, \theta_i, T\right) = \frac{Z_1 Z_2 e^2}{R(T)} + 3Z_1 Z_2 e^2 \sum_{i,i=1,2} \frac{R_i^{\lambda}(\alpha_i T)}{(2\lambda+1)R(T)^{\lambda+1}}$$

$$Y_\lambda^{(0)}(\theta_i)\left[\beta_{\lambda i} + \beta_{\lambda i}^2 Y_\lambda^{(0)}(\theta_i)\right] \qquad (2.14)$$

with the radius vector given by Eq. (2.6) and surface thickness parameter

$$b(T) = 0.99(1 + 0.009T^2). \qquad (2.15)$$

The angular momentum potential, (see section 2.3.5)

$$V_l(R, A_i, \beta_{\lambda i}, \theta_i, T) = \frac{\hbar^2 l(l+1)}{2Is(T)} \qquad (2.16)$$

with the moment-of-inertia,

$$I_s(T) = \mu R^2 + \frac{2}{5}A_1 m R_1^2(\alpha_1, T) + \frac{2}{5}A_2 m R_2^2(\alpha_2, T).$$

Further, in Eq. (2.12), within the Strutinsky renormalization procedure, we have defined the binding energy B of a nucleus at temperature T as the sum of liquid drop energy $V_{LDM}(T)$ and shell correction $\delta U(T)$ i.e

$$B(T) = V_{LDM}(T) + \delta U \exp\left(\frac{-T^2}{T_0^2}\right) \qquad (2.17)$$

The T dependent liquid drop part of the binding energy VLDM(T) is from Davidson et al. [41], based on the semi-empirical mass formula of Seeger [46]. For the shell correction δU in Eq. (2.17), since there is no microscopic shell model known that gives the shell corrections for light nuclei, we use the empirical formula of Myers and Swiatecki [45].

The mass parameters $B_{\eta\eta}(\eta)$, representing the kinetic energy part in Eq. (2.3),are the smooth classical hydrodynamical masses

[47], given by Eq. (2.60) (in the section 2.3.6) for $\theta_1 = \theta_2 = 0^0$ and R_i taken as temperature dependent.

Finally, the l_c-value in Eq. (2.6) is the critical l-value, in terms of the bombarding energy $E_{c.m.}$, the reduced mass μ and the first turning point R_a of the entrance channel η_{in}, given by

$$l_c = R_a\sqrt{(2\mu[E_{c.m.} - V(R_a, \eta_{in}, l = 0)])}/\hbar \qquad (2.18)$$

or, alternatively, it could be fixed for the vanishing of fusion barrier of the incoming channel, called l_{fus}, or else the l-value (l_{max}) where the light-particle cross section $\sigma_{LP} \rightarrow 0$. This, however, could also be taken as a variable parameter [36,48].

2.3 Quantum Mechanical Fragmentation Theory

In QMFT [19]-[32], the essential quantities for the description of the nuclear dynamics are the potential energy surfaces and the mass parameters defining the kinetic energy of the system while the static properties of nuclear system are determined by the potential energy only. The QMFT is worked out in terms of the following collective variables:

(1) Relative separation coordinate R between the two nuclei or, in general two fragments (or, equivalently, the length parameter $\lambda = L/2R_0$, with L as the length of the nucleus and R_0 as the radius of an equivalent spherical nucleus).

(2) The deformation co-ordinates $\beta_{\lambda i}$ (λ=2,3,4…. and i=1,2) of the colliding nuclei.

(3) The orientation degrees of freedom Θ_i (i= 1,2) of the deformed nuclei(fig. 2.2)

(4) Azimuthal angle Φ between the principles planes of the two colliding nuclei.

(5) Neck parameter ε, defined by the ratio $\varepsilon = E_0/E'$ for the interaction region ($R < R_1+R_2$, R_i (i=1,2) is the radius of the two nuclei);

Where E_0 is the actual height of the barrier and E' is the fixed barrier of the two centre oscillator. ε = 0 represents a broad neck formation, whereas ε= 1

gives that the neck is fully squeezed in, corresponding to the asymptotic region ($R > R_1+R_2$).

(6) Mass and charge fragmentation co-ordinates[19],[20],[31].

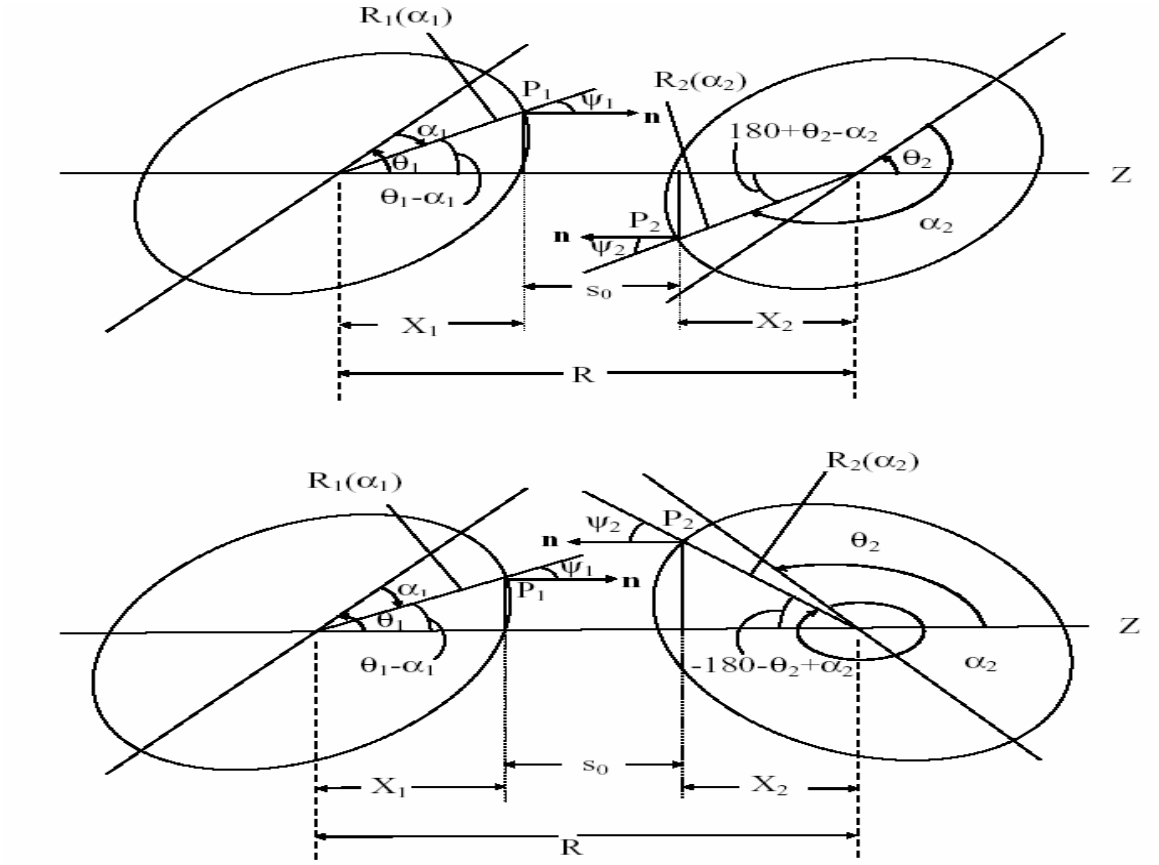

Figure 2.2: Schematic configurations of two (equal/ unequal) axially symmetric deformed, oriented nuclei, lying in the same plane and for various Θ_1 and Θ_2 values in the range 0^0 to 180^0. The Θ's are measured in anti-clockwise from the colliding axis and the angle □' s in clockwise from the symmetry axis.

For two body channels, the mass and charge fragmentations for separated nuclei/fragments are defined by the mass and charge-asymmetry coordinates as

$$\eta = \frac{A_1 - A_2}{A}; \qquad \eta_Z = \frac{Z_1 - Z_2}{Z} \tag{2.19}$$

similarly, the neutron asymmetry coordinate [20]

$$\eta_N = \frac{N_1 - N_2}{N} \tag{2.20}$$

can also be used, but it is sufficient to treat only two of them as dynamical co-ordinates since they are related as

$$\eta = \frac{Z}{A}\eta_z + \frac{N}{A}\eta_N \tag{2.21}$$

Here $A=A_1+A_2$, $Z=Z_1+Z_2$ and $N=N_1+N_2$. A_i, Z_i and N_i (i = 1, 2) are respectively the mass number, the charge number and the neutron number of two fragments. A, Z and N are respectively the mass number, charge number and neutron number of the compound nucleus system. The limiting values of η are $0 \leq |\eta| \leq 1$ and thus allows a unified description of a few – nucleon or multi - nucleon (a cluster) transfer , a large-mass transfer, the complete fusion ($|\eta| =1$) of nuclei and the symmetric ($\eta= 0$), asymmetric and super-asymmetric fission of a nucleus or compound nucleus. The η_Z coordinate gives the associated charge distribution effects. In terms of these collective coordinates and their velocities, the collective Hamiltonian can be written as(taking β to stand for $\beta_{\lambda 1}$ and $\beta_{\lambda 2}$ (λ=2,3,4….))

$$H = K(\varepsilon, \beta, \eta_z, R, \eta, \dot{\eta}_z, \dot{R}, \dot{\beta}, \dot{\eta}, \dot{\varepsilon}) + V(\varepsilon, \beta, \eta_z, R, \eta) \tag{2.22}$$

For the compound nucleus formation, the neck parameter ε=0 is assumed, since once the neck formation starts between the two colliding nuclei, then fission phenomenon takes place, i.e. excited compound nucleus will proceed towards the disintegration process.

For the potential $V(\eta, \eta_Z, R)$, minimized in the η_Z coordinate, Schrödinger wave equation in terms of mass parameters η and relative separation R co-ordinate can be written as:

$$H(\eta, R)\Psi(\eta, R) = E(\eta, R)\,\Psi(\eta, R) \quad (2.23)$$

With the Hamiltonian,

$$H(\eta, R) = K(\eta) + K(R) + K(\eta, R) + V(\eta) + V(R) + V(\eta, R) \quad (2.24)$$

Here, K refers to the kinetic energy and V to the collective potential energy. The mass parameters $B_{ij.}$ Defining the kinetic energy term K in the above Eqs.(2.24) and (2.26) are either the consistently calculated cranking masses using the Asymmetric shell model (ATCSM) or the classical hydrodynamic masses, which are shown to have good agreement with microscopic cranking calculations. The coupling term of the kinetic energy K (η,R), proportional to $\partial^2/(\partial_\eta \partial_R)$, is neglected here, since the coupled cranking masses are very small [19],[20] ($B_{R\eta} << (B_{RR}B_{\eta\eta})^{1/2}$ and $B_{R\eta Z} << (B_{RR}B_{\eta Z\eta Z})^{1/2}$). Same is true for the coupling term of potential energy V (η,R). Therefore, in a decoupled approximation [32], the Schrodinger equation (2.25) can be solved for which the Hamiltonian takes the form:

$$H = \frac{-\hbar^2}{2\sqrt{B_{\eta\eta}}}\frac{\partial}{\partial_\eta}\frac{1}{\sqrt{B_{\eta\eta}}}\frac{\partial}{\partial_\eta} - \frac{\hbar^2}{2\sqrt{B_{RR}}}\frac{\partial}{\partial_R}\frac{1}{\sqrt{B_{RR}}}\frac{\partial}{\partial_R} + v(\eta) + v(R) \quad (2.25)$$

For decoupled Hamiltonian (2.7), Schrödinger wave equation (2.23) can be separated for the two co-ordinates η and R as follows,

$$\left[\frac{-\hbar^2}{2\sqrt{B_{\eta\eta}}}\frac{\partial}{\partial_\eta}\frac{1}{\sqrt{B_{\eta\eta}}}\frac{\partial}{\partial_\eta} + v(\eta)\right]\Psi^v(\eta) = E_\eta^v\Psi^v(\eta) \quad (2.26)$$

$$\left[\frac{-\hbar^2}{2\sqrt{B_{RR}}}\frac{\partial}{\partial_R}\frac{1}{\sqrt{B_{RR}}}\frac{\partial}{\partial_R} + v(R)\right]\Psi^v(R) = E_R^v\Psi^v(R) \quad (2.27)$$

With $\psi(\eta,R) = \psi(\eta)\psi(R)$ (2.28)

$$E = E_\eta + E_R \quad (2.29)$$

The states $\Psi^v(\eta)$ are the vibrational states in the potential V(η) and are labeled by the quantum numbers ν =0,1,2……

In the following subsections, we first discuss the various the various terms of schrodinger wave equations (2.26) and (2.27) and then give the solution of Eq. (2.26) for the determination of preformation probability $P_0 \propto |\psi^0(\eta)|^2$.

2.3.1 The Scattering Potential V(R)

For a fixed η i.e. for a given outgoing fragment (A_1,A_2) combination, the scattering potential V(R) in Eq. (2.27) is defined as the sum of the deformations, orientations dependent coulomb potential, proximity potential and angular momentum dependent potential, i.e.

$$V(R) = V_c(R, Z_i, \beta_{\lambda i}, \theta_i, \Phi) + V_p(R, A_i, \beta_{\lambda i}, \theta_i, \Phi) + V_\ell(R, A_i, \beta_{\lambda i}, \theta_i, \Phi) \quad (2.30)$$

2.3.2 The Fragmentation potential V(η)

The collective potential energy or the fragmentation potential V(η,R), appearing in equation (2.8) is calculated as,

$$V(\eta,R) = -\sum_{i=1}^{2} Bi(Ai, Zi\ \beta\lambda i) + Vc(R, Zi, \beta\lambda i, \theta i, \varphi) + Vp(R, Ai, \beta\lambda i, \theta i, \varphi) + V_l(R, Ai, \beta\lambda i, \theta i, \varphi) \quad (2.31)$$

Here B_i (i=1,2) are the binding energies of the two nuclei, available from the experimental data of Audi-wapstra [43]. Wherever the experimental B's are not available, the theoretical binding energies of Moller et al.[44] are used. Note that the binding energies contain both the macroscopic (liquid drop part) and the microscopic (shell correction part).

The fragmentation potential V (η) is calculated at a fixed distance $R=R_1+R_2+\delta R$ or $R=C_1+C_2+\delta C$ fm, with C_i (i=1,2) as the sussmann central radii related to the radius vector R_i as $C_i = R_i(1 - b^2/R_i^2)$ with

$$R_i = R_{0i}[1+\sum_\lambda \beta\ \lambda i\ Y_\lambda^{(0)}(\alpha i)\ ], \quad (2.32)$$

and

$$R_{0i} = 1.28A_i^{1/3} - 0.76 + 0.8A_i^{-1/3} \quad (2.33)$$

Here λ=2,3,4…. and α_i is an angle that the radius vector R_i of the colliding nuclei makes with the symmetry axis(fig.2.2) the diffuseness of the nuclear surface (I.e. the surface thickness) b = 0.99 fm. The charges Z_i are fixed by minimizing the potential V (η) in the η_Z coordinate at each η value.

For the study of excited systems, where the nuclear temperature effects also come into picture, the fragmentation potential at fixed R is

$$V(\eta, T) = \sum_{i=1}^{2} V_{LDM}(A_i, Z_i, T) + \sum_{i=1}^{2} \delta U \exp(-T^2/T^2_0) + V_c(Z_i, \beta_{\lambda i}, \theta_i, \varphi, T) + V_p(A_i, \beta_{\lambda i}, \theta_i, \varphi, T) + V_i(A_i, \beta_{\lambda i}, \theta_i, \varphi, T) \quad (2.34)$$

Here, V_{LDM} (A_i, Zi, T) is the liquid drop part of the binding energy and δU, the shell corrections. Note that the calculation of fragmentation potential involves all the possible decay channels and the number of all such possible decay channels becomes more and more with the increasing mass of the mother nucleus. The nuclear temperature T (in MeV) is related to the excitation energy E^*_{CN} of the compound nucleus, through a semi-empirical statistical relation as:

$$E^*_{CN} = 1/10AT^2 - T \ \text{(MeV)} \quad (2.35)$$

The shell corrections δU in Eq. (2.34) are considered to vanish exponentially for $E^*_{CN} \geq 60$ MeV , giving $T_0 = 1.5$ MeV . At higher excitation energies the shell corrections vanish completely and only the liquid drop part of energy is present. The shell corrections play an important role in determining or empirical fitting of nuclear masses, because the nuclear masses calculated by using the smooth liquid drop formula show large deviations with respect to the experimental masses. It means that in the experimental masses there exist deep minima at specific neutron and/or proton numbers indicating the presence of shell structure, the so-called magic numbers in nuclei. This characteristic behavior cannot be reproduced by the liquid drop part alone, which means that the introduction of microscopic shell correction in the mass formula is essential. Thus, shell corrections accounts for the removal of deviation from the liquid drop calculations (uniform distribution of nucleons), and are defined, within Strutinsky [49] method as

$$\delta U = U - \tilde{U} \quad (2.36)$$

where, $U = \sum_\nu E_\nu 2n_\nu$ is the sum over all occupied single particle states and

$$\tilde{U} = \int_{-\infty}^{\tilde{\lambda}} E\tilde{g}(E)dE \qquad (2.37)$$

is the average energy for uniform distribution. In general, the microscopic shell correction, together with the liquid drop part, gives a proper description of the binding energy of the nucleus. This method, however, does not give a proper description of light mass nuclei. The difficulty is the inadequacy of shell model for very light nuclei. For this reason, the macro-microscopic calculations of Moller et al. [44] are tabulated for Z ≥ 8 only. For Z ≤ 8, one could alternatively use the empirical shell correction method of Myers-Swiatecki [38] which again is not very satisfactory for light nuclei (Z ≤ 16). Gupta and collaborators have modified this empirical method and obtained a better description of the shell corrections for the light as well as heavy mass region, i.e,1 ≤ Z ≤ 118 [4].

2.3.3 The Proximity Potential for Deformed, Oriented and Coplanar Nuclei

When two surfaces approach each other within a small distance of less than ~ 2fm, comparable with the surface thickness of interacting nuclei, or when a nucleus is at the verge of dividing into two fragments, then the two surfaces actually face each other across a small gap or crevice. In both cases, the surface energy term alone could not give rise to the strong attraction that is observed when the two surfaces are brought in close proximity. Such additional attractive forces are called proximity forces and the additional potential due to these forces is called the nuclear proximity potential.

Blocki et al. [50] have reanalyzed and extended a theorem, originally due to

Deryagin [51], according to which the force between two gently curved surfaces in close proximity is proportional to the interaction potential per unit area between the two flat surfaces. The original expression of Blocki based on the pocket formula was for spherical nuclei, and is given as

$$V_P(s_0) = 4\pi\bar{R}\gamma\, b\, \Phi(s_0). \quad (2.38)$$

$\Phi(s_0)$ is the universal function, independent of the shapes of nuclei or the geometry of nuclear system, but depends on the minimum separation distance

$$\Phi(s_0) = \begin{cases} -1/2(s_0 - 2.54)^2 - (s_0 - 2.54)^3 \\ -3.437\exp(-s_0/0.75) \end{cases} \quad (2.39)$$

respectively, for $s_0 \leq 1.2511$ and $s_0 \geq 1.2511$. Here, s_0 is defined in units of b, i.e. s_0 is s_0/b. This function is defined for negative (the overlap region), zero (touching configuration) and positive values of s_0. For a fixed R, the minimum distance s_0 for spherical nuclei is defined as

$$s_0 = R - R_1 - R_2 \quad (2.40)$$

where $R = 1.07A_i^{1/3}(i=1,2)$. b is the diffuseness of the nuclear surface given by

$$b=[\pi/2\sqrt{3}\ln 9]\, t_{10\text{-}90} \quad (2.41)$$

where $t_{10\text{-}90}$ is the thickness of the surface in which the density profile changes from 90% to 10%. The value of b ~1 fm. The γ is the specific nuclear surface tension given by

$$\gamma = 0.9517[1-1.7826(N-Z/A)^2] \text{ Mev fm}^{-2} \quad (2.42)$$

R' is the mean curvature radius of the reaction partners, characterizing the gap, which for spherical nuclei is given by

$$\bar{R} = R_1R_2 / R_1 + R_2 \quad (2.43)$$

2.3.4 The Coulomb Potential

Coulomb potential describes the force of repulsion between two interacting nuclei due to their charges. It acts along the line joining the two nuclei. The Coulomb

potential for two interacting spherical nuclei is given as

$$V_c = Z_1 Z_2 e^2 / R \qquad (2.44)$$

For interacting deformed and oriented nuclei, different authors [54]-[58] have derived it differently. In this thesis work, we have started with Coulomb potential of Wong [57], given for two non-overlapping charge distributions, having qudarupole deformations only, i.e.,

$$V_c = \frac{Z_1 Z_2 e^2}{R} + \left(\frac{9}{20\pi}\right)^{1/2} \left(\frac{Z_1 Z_2 e^2}{R^3}\right) \sum_{i=1}^{2} R_i^2(\alpha_i)\beta_{2i} P_2(cos\theta_i) + \left(\frac{3}{7\pi}\right) \left(\frac{Z_1 Z_2 e^2}{R^3}\right) \sum_{i=1}^{2} R_i^2(\alpha_i) \left[\beta_{2i} P_2(cos\theta_i)\right]^2 \qquad (2.45)$$

In this expression, the quadrupole-quadrupole interaction term, proportional to $\beta_{21}\beta_{22}$, is neglected since it has a short-range character. For nuclei lying in the same plane we have generalized it to include the higher order deformations (λ = 3, 4...), obtaining

$$V_c(Z_i, \beta_{\lambda i}, \theta_i, T) = \frac{Z_1 Z_2 e^2}{R(T)} + 3 Z_1 Z_2 e^2 \sum_{\lambda, i=1,2} \frac{R_i^{\lambda}(d_i, T)}{(2\lambda+1) R(T)^{\lambda+1}} \left[\beta_{\lambda i} + \beta_{\lambda i}^2 Y_{\lambda}^{(0)}(\theta_i)\right] \qquad (2.46)$$

With Ri from eq (2.32) $Y_{\wedge}^{(0)}(\Theta_i)$ are the spherical harmonic function.

2.3.5 **Rotational Energy Due to Angular Momentum**

The rotational motion gives an additional energy due to the angular momentum define as

$$V_l = \frac{\hbar^2 l(l+1)}{8\pi^2 I} \qquad (2.47)$$

with $I = \mu R^2$, is the non-sticking limit of moment of inertia with as the $\mu = \frac{A1A2}{A1+A2} m$ reduced mass. m is the nucleon mass. In the complete sticking limit, the moment of inertia I is given as,

$$I = \mu R^2 + 2/5 A_1 m R^2_1 + 2/5 A_2 m R^2_2 \quad (2.48)$$

with R_i from Eq. (2.32). However, for the relative separation of interest here, we use the sticking limit. It is relevant to mention here that value of angular momentum extracted experimentally, is based upon moment of inertia limit. [59]

2.3.6 Classical Hydrodynamic Mass Parameters

The kinetic energy part of the Hamiltonian in Eq. (2.26) enters through the mass parameters. We use here the classical mass parameters of Kroger and Scheid [47]. The model of Kroger and Scheid is based on the hydrodynamic flow, as shown in Fig. 2.3. This model gives a simple analytical expression, whose predictions are shown to compare nicely with the microscopic cranking model calculations. For the $B_{\eta\eta}$ mass we get

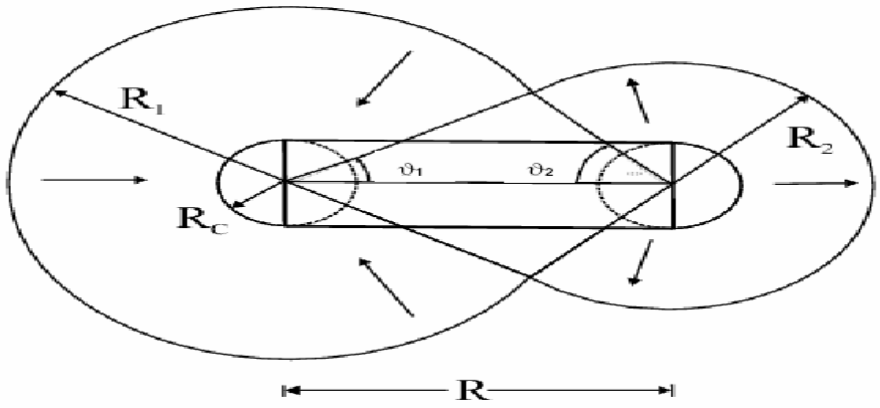

$$B\eta\eta = \frac{AmR2}{4}\left[\frac{vt(1+}{vc1+\left(\frac{vt(}{vc(1}\right.}\right.$$

(2.49)

With

$$\gamma = = \frac{Rc}{2R}\left[\frac{1}{1+\cos \square 1}(1\right.$$

(2.50)

$$\delta = \frac{1}{2R}[(1 - \cos \square_1)+(1 - \cos \square_2)]$$

(2.51)

$$v_c = \pi^2 R^2_c R \quad (2.52)$$

Fig. 2.3 The geometry of classical hydrodynamic model for calculating mass parameter $B_{\eta\eta}$

and $v_t = v_1+v_2$, is the total conserved volume. The angles θ_1 and θ_2 and geometry of the model are shown in Fig. 2.3. For $\theta_1 = \theta_2 = 0$, $\delta = 0$ which corresponds to two touching spheres. R_c(is not equal to 0) is the radius of a cylinder of length R, having a homogeneous flow in it; whose existence is assumed for the mass transfer between the two spherical fragments. We have generalized this formalism for deformed nuclei by using the radii R_1 and R_2 for deformed nuclei, given by Eq. (2.32).

2.3.7 Solution of the Schrödinger Equation and the Fragments Preformation Probability P_0

Once the Hamiltonian Eq. (2.25) is established, the Schrödinger equation in mass fragmentation co-ordinate η can be solved. On solving Eq. (2.26) numerically, $|\psi^v(\eta)|^2$ gives the probability P_0 of finding the mass fragmentation η at a fixed R on the decay path.

$$P_0(A_2)=|\psi^v(A_2)|^2 \qquad (2.53)$$

For fission studies, like the spontaneous fission and fission through the barrier, the motion in R at the saddle point is adiabatically slow as compared to the η motion. Therefore, the potential is minimized in the neck and deformation coordinates $ß_1$ and $ß_2$ at each R and η values. Starting from the nuclear ground state in spontaneous fission or cluster decay, and to have complete adiabaticity,

only the lowest vibrational state $\nu = 0$ is occupied. Then, the mass (or charge) distribution yield, proportional to the probability $|\psi^{(0)}(\eta)|^2$ or $|\psi^{(0)}(\eta_z)|^2$ of finding a certain mass (or charge) fragmentation η (or η_z) at a position R on the decay path, when scaled to, say, mass A_2 of one of the fragments ($d\eta = 2/A$) is given by:

$$Y(A_2) = |\psi_R^{(0)}(A_2)|^2 \frac{2}{A} \sqrt{B_{\eta\eta}(A_2)}). \tag{2.54}$$

However, if the system is excited or we allow interaction between various degrees of freedom, higher values of ν would also contribute. These enter via the excitation of higher vibrational states, and through the temperature dependent potential V and masses B_{ij} The effect of adding temperature on potential V and masses B_{ij} is to reduce the shell effects in them, resulting finally in the liquid drop potential V_{LDM} and smoothed (averaged) masses B_{ij} for the systems to be very hot. Apparently, cold fission means taking both the potential V and masses B_{ij} with full shell effects included in them and hot fission means using the V_{LDM} and smoothed (averaged) masses B_{ij}. The possible consequence of such excitations are included here by assuming a Boltzmann like occupation of excited states

$$|\psi(\eta)|^2 = \sum_{\nu=0}^{\infty} |\psi^{\nu}(\eta)|^2 \exp\left(-\frac{E_\eta^\nu}{T}\right) \tag{2.55}$$

Note that we are dealing here with a directly measurable quantity, the mass (or charge) asymmetry, which works dynamically as mass (or charge) transfer coordinate. Thus, the calculated yields Y (A_i) (or Y (Z_i)) are directly comparable with experiments. It may be stressed that there is no free parameter in these calculations. The nuclear shape, once minimized in the neck and deformation coordinates $ß_1$ and $ß_2$ at a given R ($=R_{saddle}$), remains fixed for both the mass and charge distributions of fission or decay fragments.

2.4 Penetration Probability P

Penetrability P measures the of capability of fragments nucleus to penetrate the potential barrier generalized during compound nucleus formation

2.5 Assault Frequency ν_0

For the cluster decay studies in the following section, another quantity of interest is the assault frequency ν_0 defined as,E_2

$$\nu_0 = \frac{v}{R0} = \frac{\sqrt{(2E_2/\mu)}}{R0} \tag{2.56}$$

where R_0 is the radius of parent nucleus and $E_2 = 1/2\mu v^2$ is the kinetic energy of the emitted cluster. Since both the emitted cluster and the daughter nucleus are produced in the ground state, the entire positive Q-value is the total kinetic energy ($Q = E_1 + E_2$) available for the decay process, which is shared between two fragments, such that for the emitted cluster

$$E_2 = (\frac{A_1}{A})Q \tag{2.57}$$

and, $E_1 = Q - E_2$ is the recoil energy of the daughter nucleus.

REFERENCES:

[1] R.K. Gupta, M. Balasubraniam, C. Mazzocchi, M. La Commara, and W. Scheid, Phys. Rev. C 65, 024601 (2002).

[2] M.K. Sharma, R.K. Gupta, and W. Scheid, J. Phys. G 26, L45 (2000).

[3] R.K. Gupta, R. Kumar, N.K. Dhiman, M. Balasubraniam, W. Scheid, and C. Beck, Phys. Rev. C 68, 014610 (2003).

[4] M. Balasubraniam, R. Kumar, R.K. Gupta, C. Beck, and W. Scheid, J. Phys. G 29, 2703 (2003): R.K. Gupta, M.K. Sharma and B. Singh, Phys. Rev. C-to be published

[5] R.K. Gupta, M. Balasubraniam, R. Kumar, D. Singh, and C. Beck, Nucl. Phys. A 738, 479c (2004).

[6] R.K. Gupta, M. Balasubramaniam, R. Kumar, D. Singh, C. Beck, and W. Greiner, Phys. Rev. C 71, 014601 (2005).

[7] B.B. Singh, M.K. Sharma, R.K. Gupta, and W.Greiner,Int.J. Mod.Phys.E15, 699 (2006)

[8] R.K. Gupta, M. Balasubraniam, R.Kumar, D.Singh ,S. K. Arun and W.Greiner,J.Phys .G:Nucl.Part. Phys. 32, 345(2006)

[9] B.B. Singh, M.K. Sharma, R.K. Gupta,Phys.Rev. C 77, 054613 (2008)

[10] R.Gupta, in proceedings of the 5th International Conference on Nuclear Research Mechanics, Varenna, 1988, edited by E. gladioli , (Ricerca Scientifica ed Educazione Permanente ,Milano, 1988),p.416.

[11] S.S. Malik and R.K.Gupta, Phys.Rev.C 39, 1992(1989)

[12] R.K.Gupta, W.Scheid, and W.Greiner, J.Phys.G:Nucl. Part. Phys. 17, 1731(1991).

[13] S. Kumar and R.K.Gupta, Phys.Rev. C 49, 1922(1994).

[14] R.K.Gupta and W. Greiner Int. J. Mod. Phys. E 3, 335 (1994, Suppl.).

[15] S. Kumar and R.K.Gupta, Phys. Rev. C 55, 218 (1997).

[16] R.K. Gupta, in Heavy Elements and Related New Phenomena ,edited by W.Greneir and R.K Gupta (World Scientific Singapore) Vol.II ,p.730

[17] S.K and R.K Gupta ,DAE nucl.Phys.(Sambalpur)52,365(2007)

[18] B.B.Singh,S.K Arun, M.K.Sharma , S.Kanwar and Raj K.Gupta ,DAE Nucl.Phys.(Roorkee), Accepted(2008)

[19] J. Maruhn and W. Greiner, Phys. Rev. Lett. 32, 548 (1974).

[20] R.K. Gupta, W. Scheid and W. Greiner, Phys. Rev. Lett. 35, 353 (1975).

[21] A. S¡andulescu, R.K. Gupta, W. Scheid and W. Greiner, Phys. Lett. 60B, 225 (1976).

[22] R.K. Gupta, A. S¡andulescu and W. Greiner, Phys. Lett. 67B, 257 (1977); Rev. Roum. Phys. 23, 51 (1978).

[23] S. Yamaji, W. Scheid, H.J. Fink and W. Greiner, Z. Phys. A 278, 69 (1976).

[24] S. Yamaji, W. Scheid, H.J. Fink and W. Greiner, J. Phys. G: Nucl. Phys. 2, L189 (1976).

[25] S. Yamaji, K.H. Ziegenhain, H.J. Fink, W. Greiner and W. Scheid, J. Phys. G: Nucl. Phys. 3, 1283 (1977).

[26] R.K. Gupta, A. S¡andulescu and W. Greiner, Z. Naturforsch. 32a, 704 (1977).

[27] R.K. Gupta, C. Pirvulescu, A. S¡andulescu and W. Greiner, Z. Phys. A 283, 217 (1977); Sovt. J. Nucl. Phys. 28, 160 (1978).

[28] R.K. Gupta, Z. Physik. A 281, 159 (1977).

[29] A. S¡andulescu, H.J. Lustig, J. Hahn, and W. Greiner, J. Phys. G: Nucl. Phys.4, L279 (1978).

[30] H.J. Lustig, J.A. Maruhn, and W. Greiner, J. Phys. G: Nucl. Phys. 6, L25(1980).

[31] H.J. Fink and W. Greiner and R.K. Gupta and S. Liran and J.H. Maruhn and W. Scheid and O. Zohni, in Proceedings of Int. Conf. on Reaction between Complex Nuclei, Nashville, 1974, 21, (Amsterdam: North Holland), pages 2.

[32] R. K. Gupta, IANCAS Bull. (India), 6, 2(1990).

[33] R.K. Gupta, N.Singh, and M. Manhas, Phys. Rev. C 70, 034608 (2004)

[34] R.K. Gupta ,M.balasubramaniam, R.Kumar, N.Singh, M.Manhas, and W. Greiner, J.Phjs. G: Nucl.Part. Phys. C 31, 631(2005).

[35] T. Matsuse, C. Beck, R. Nouicer, and D. Mahboub, Phys. Rev. C 55, 1380 (1997).

[36] S.J. Sanders, D.G. Kovar, B.B. Back, C. Beck, D.J. Henderson, R.V.F. Janssens, T.F. Wang, and B.D. Wilkins, Phys. Rev. C 40, 2091 (1989t).

[37] S.J. Sanders, Phys. Rev. C 44, 2676 (1991).

[38] J. Gomez del Campo, R.L. Auble, J.R. Beene, M.L. Halbert, H.J. Kim, A. D'Onofrio, and J.L. Charvet, Phys. Rev. C 43, 2689 (1991); Phys. Rev. Lett. 61, 290 (1988).

[39] R.J. Charity, M.A. McMahan, G.J. Wozniak, R.J. McDonald, L. G. Moretto, D.G. Sarantites, L.G. Sobotka, G. Guarino, A. Pantaleo, L. Fiore, A. Gobbi and K.D. Hildenbrand, Nucl. Phys. A 483, 371 (1988).

[40] C. Beck, R. Nouicer, D. Disdier, G. Duchˆene, G. de France, R.M. Freeman, F. Haas, A. Hachem, D. Mahboub, V. Rauch, M. Rousseau, S.J. Sanders, and A. Szanto de Toledo, Phys. Rev. C 63, 014607 (2001).

[41] N.J. Davidson, S.S. Hsiao, J. Markram, H.G. Miller, and Y. Tzeng, Nucl. Phys. A 570, 61c (1994).

[42] G. Audi and A.H. Wapstra, Nucl. Phys. A 595, 4 (1995).

[43] G. Audi and A.H. Wapstra and C. Thiboult, Nucl. Phys. A 729, 337(2003)

[44] P. M¨oller, J. R. Nix, W. D. Myers, and W. J. Swiatecki, At. Data Nucl. Data Tables 59, 185 (1995).

[45] W. Myers and W.J. Swiatecki, Nucl. Phys. 81, 1 (1966).

[46] P. A.Seeger, Nucl. Phys. 25, 1 (1961)

[47]H.Kroger and W. Scheid, J. Phys. G 6, L85(1980)

[48] S.J. Sanders, D.G. Kovar, B.B. Back, C. Beck, B.K. Dichter, D. Henderson, R.V.F. Janssens, J.G. Keller, S. Kaufman, T.-F. Wang, B. Wilkins, and F. Videbaek, Phys. Rev. Lett. 59, 2856 (1987).

[49] V.M. Strutinsky, Nucl. Phys. A 95, 420 (1967).

[50] J. Blocki, J. Randrup, W. J. Swiatecki, and C. F. Tsang, Ann. Phys. (NY) 105, 427 (1977).

[51] Deryagin, Kolloid Z. 69, 155 (1934).

[52] A. Gray, Modern Di_erential Geometry of Curves and Surfaces with Mathe-

matica, 2nd Edition, CRC Press, Boca Raton, 1997, p.89.

[53] M. Seiwert, W. Greiner, V. Oberacker, and M.J. Rhoades-Brown, Phys. Rev. C 29, 477 (1984).

[54] N. Malhotra and R.K. Gupta, Phys. Rev. C 31, 1179 (1985).

[55] M M¨unchow, D Hahn and W Scheid, Nucl. Phys. A 388, 381 (1982).

[56] M J Rhoades-Brown, V E Oberacker, M Seiwert and W Greiner, Z. Phys. A 310, 287 (1983).

[57] C Y Wong, Phys. Rev. Lett. 31, 766 (1973).

[58] R Aroumougame and R K Gupta, J. Phys. G: 6, L155 (1980).

[59]S.Kailais(private communication)

CHAPTER 3

Entrance Channel Effect in $^{82}Sr^*$ Using Dynamic Cluster Decay Model

3.1 DCM Results

The decay of the $^{82}Sr^*$ nucleus, formed in entrance channel reactions $^{16}O+^{66}Zn$ and $^{37}Cl+^{45}Sc$ at different incident energies, is studied by using the Dynamical Cluster Decay model (DCM) extended to include the deformations and orientations of nuclei. The data is available for quasi fission (preformation probability $P_0=1$) and evaporation residue ($A_2 \leq 4$) process for this nuclear system. The decay fragments are calculated as emissions of preformed clusters through the interaction barriers. The DCM calculations for asymmetric $^{16}O + {}^{66}Zn$ at different $E_{c.m}$ values as shown in table 3.1.This table shows the data for $^{16}O+^{66}Zn$ channel at different center of mass energies i.e at different temperatures. The DCM calculated [2-10] cross section is formed to be at good agreement in the available experimental data. The ΔR and ℓ_{max} values are also given for drawing comparative study with $^{37}Cl+^{45}Sc$ channel.

$E_{c.m}$(Mev)	Temperature (MeV)	E xperimental		DCM		ΔR_{NCN}	ΔR_{CN}	ℓ_{max}
		σ_{NCN}	σ_{CN}	σ_{NCN}	σ_{CN}			
50.5768	2.435	164±10	857	165	862	1.283	1.59	57
54.6768	2.532	214±9	981	222	977.5948	1.293	1.631	59
58.8768	2.625	228±11	1079	225	1075.29	1.269	1.67	61
62.9768	2.708	324±13	1157	324	1160.611	1.374	1.688	59
67.0768	2.793	304±11	1219	302	1217	1.425	1.644	57
71.1768	2.873	308±16	1240	308	1232.467	1.445	1.73	57
76.1768	2.970	319±19	1255	317	1258.3	1.471	1.598	57

Table 3.1 Comparison of DCM calculated σ_{CN} and σ_{NCN} for $^{16}O+^{66}Zn$ reaction channel in the experimental data [1]

$E_{c.m}$(Mev)	Temperature (Mev)	E xperimental		DCM		ΔR_{NCN}	ΔR_{CN}	ℓ_{max}
		σ_{NCN}	σ_{CN}	σ_{NCN}	σ_{CN}			
60.0825	2.577	34±5	354	33.1	358	1.51	1.449	54
64.3825	2.669	51±5	540	51.7	537	1.335	1.6105	57
68.7825	2.760	66±7	690	66.9	696	1.393	1.602	57
73.1825	2.847	104±12	824	102.0	823.4	1.603	1.678	55

Table 3.2 comparison of DCM calculated σ_{CN} and σ_{NCN} for $^{37}Cl+^{45}Sc$ reaction channel in the experimental data [1]

The result of relatively symmetric entrance channel $^{37}Cl+^{45}Sc$ are given in table 3.2. Table 3.2 shows DCM result for by $^{37}Cl+^{45}Sc$ channel of different center of mass energies i.e different temperatures along with experimental data. Clearly DCM calculations are found to be in good agreement with experimental data. The ΔR and ℓ_{max} values are given for the reason stated above.

The comparative behavior in Table 3.1 and 3.2 clearly indicate that the fraction of total reaction cross section in $^{16}O+^{66}Zn$ where as the $^{37}Cl+^{45}Sc$ channel gives mainly compound nucleus products. In other words quasi fission is more

predominate in $^{16}O+^{66}Zn$ channel as compared to $^{37}Cl+^{45}Sc$ reaction channel. More predominate mode of fission is by evaporation residue formation.

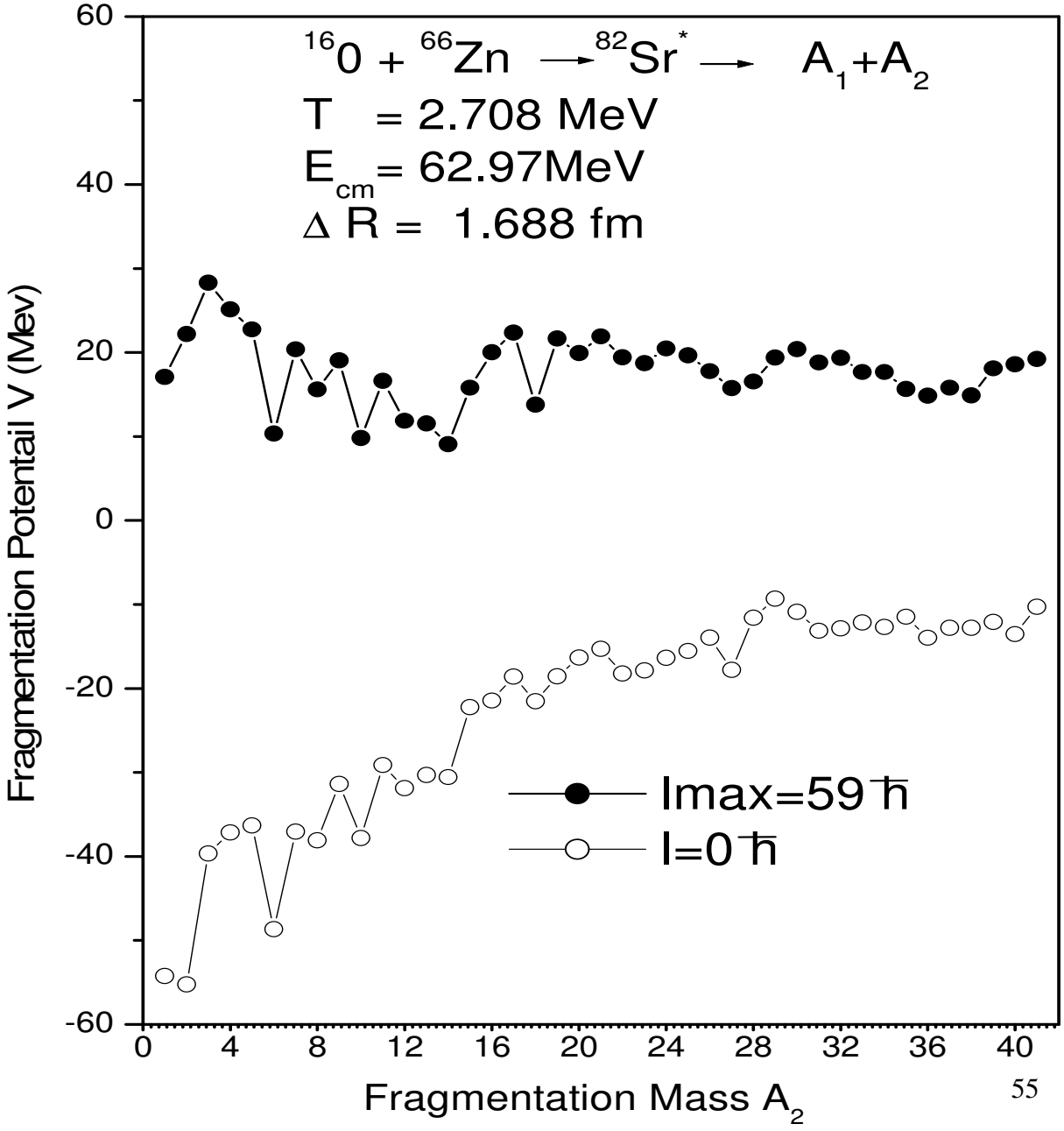

Fig.3.1 Fragmentation Potential as a function of fragment mass A_2 for $^{16}O+^{66}Zn\rightarrow {}^{82}Sr^{*}\rightarrow A_1+A_2$ reaction.

In fig.3.1 the behavior of fragmentation potential with fragmentation mass number $1 \leq A_2 \leq 81$ is shown at $E_{c.m}$ = 62.9768 MeV, T=2.708 MeV, ΔR= 1.688 fm for $^{16}O+^{66}Zn$rection at two extreme ℓ values. An α- nuclear structure is evident at both angular momentum values as expected. At ℓ=0 Evaporation Residue process seem to be dominant where as higher ℓ-values ($\ell = \ell_{max}$=59ħ) fission/Quasi fission seems to be competing with Evaporation residue process

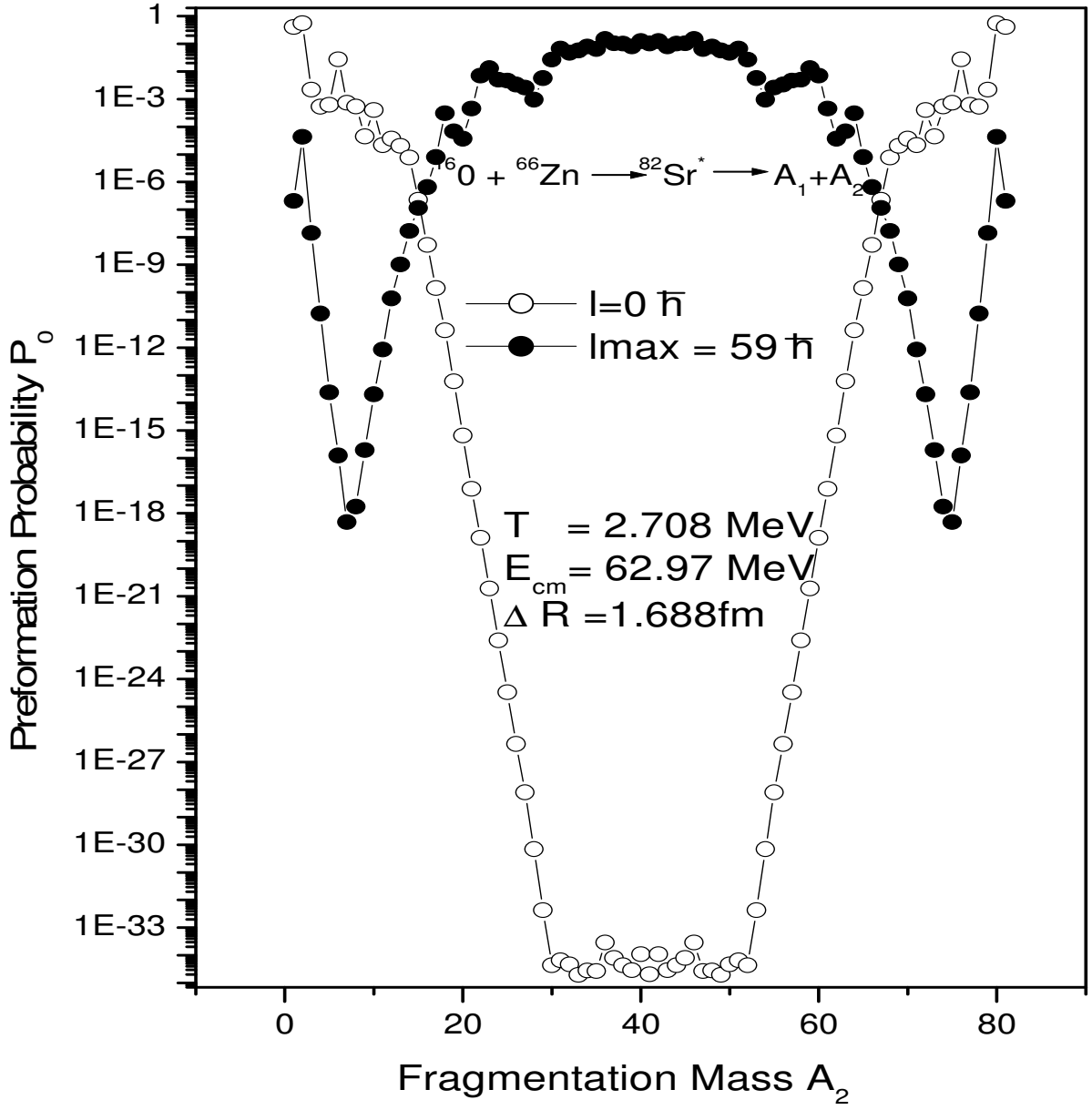

Fig.3.2 Preformation Probability as a function of fragment mass A_2 for $^{16}O+^{66}Zn\rightarrow {}^{82}Sr^*\rightarrow A_1+A_2$ reaction.

In Fig.3.2 Preformation Probability P_0 is plotted as a function of fragmentation mass for $^{16}O+^{66}Z$nchannel for same parameter as taken in Fig3.1. Preformation Probability P_0 at $\ell = 0\hbar$ is higher for $0\leq A_2\leq 4$(light particles) as compared to symmetric and near symmetric fragments. On the contrary we find that probability become prominent for symmetric and near symmetric fragments as compared to light particles. The interesting feature of the study is that behavior shift from asymmetric fragments to symmetric fragment with increase in ℓ- values.

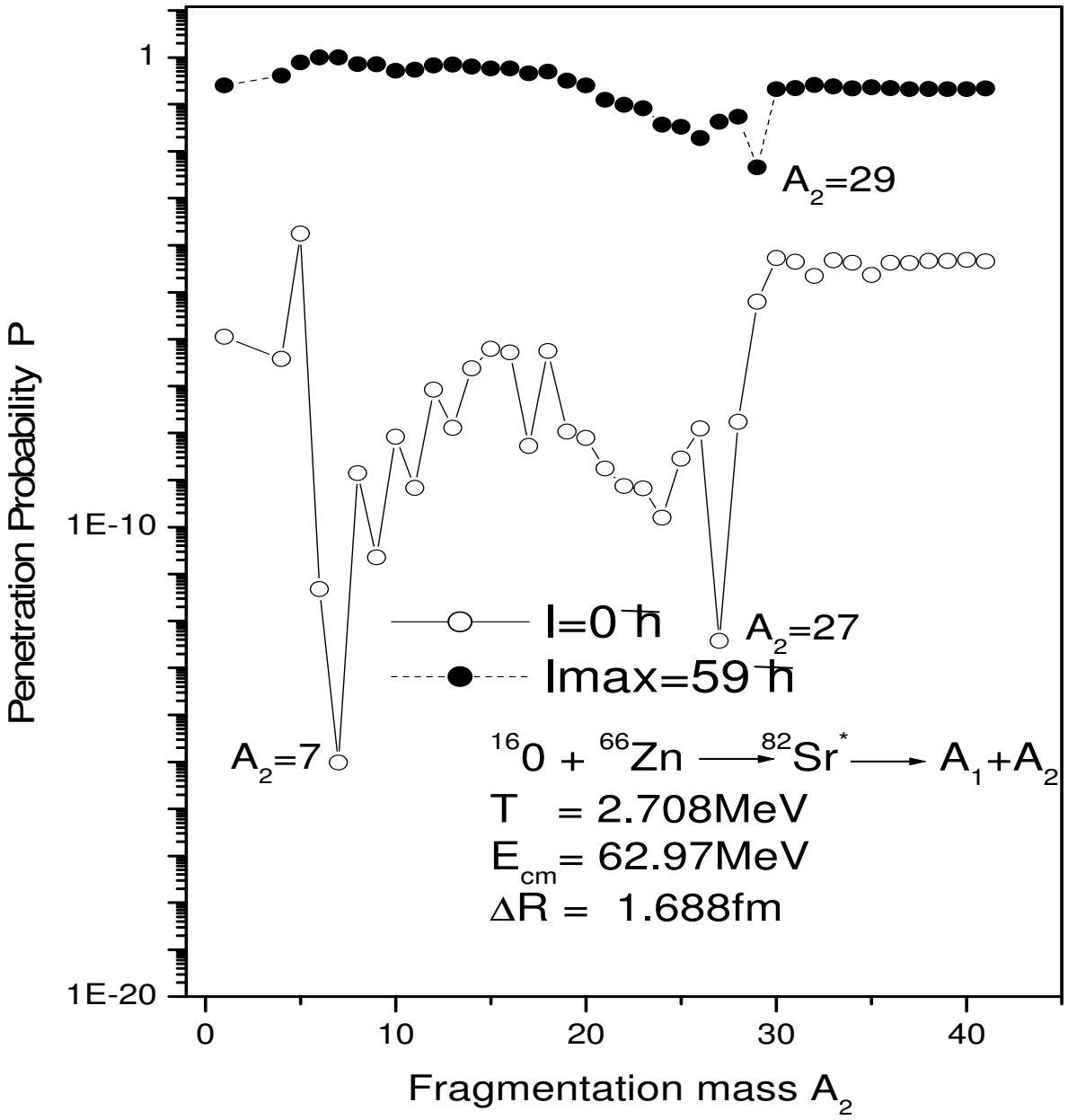

Fig.3.3 Penetration Probability as a function of fragment mass A_2 for $^{16}O+^{66}Zn \rightarrow {}^{82}Sr^{*} \rightarrow A_1+A_2$ reaction.

Penetrability P measures the of capability of fragments nucleus to penetrate the potential barrier generalized during compound nucleus formation. Variation of penetration probability P with fragmentation mass A_2 is given for system $^{16}O + {}^{66}Zn$ reaction channel. The penetrability shows interesting structure for the lower ℓ &intermediate mass fragment at ℓ=0value, and become almost constant for high mass fragments. On the contrary penetrability remain almost constant for high ℓ-value, ℓ_{max}=59ħ.

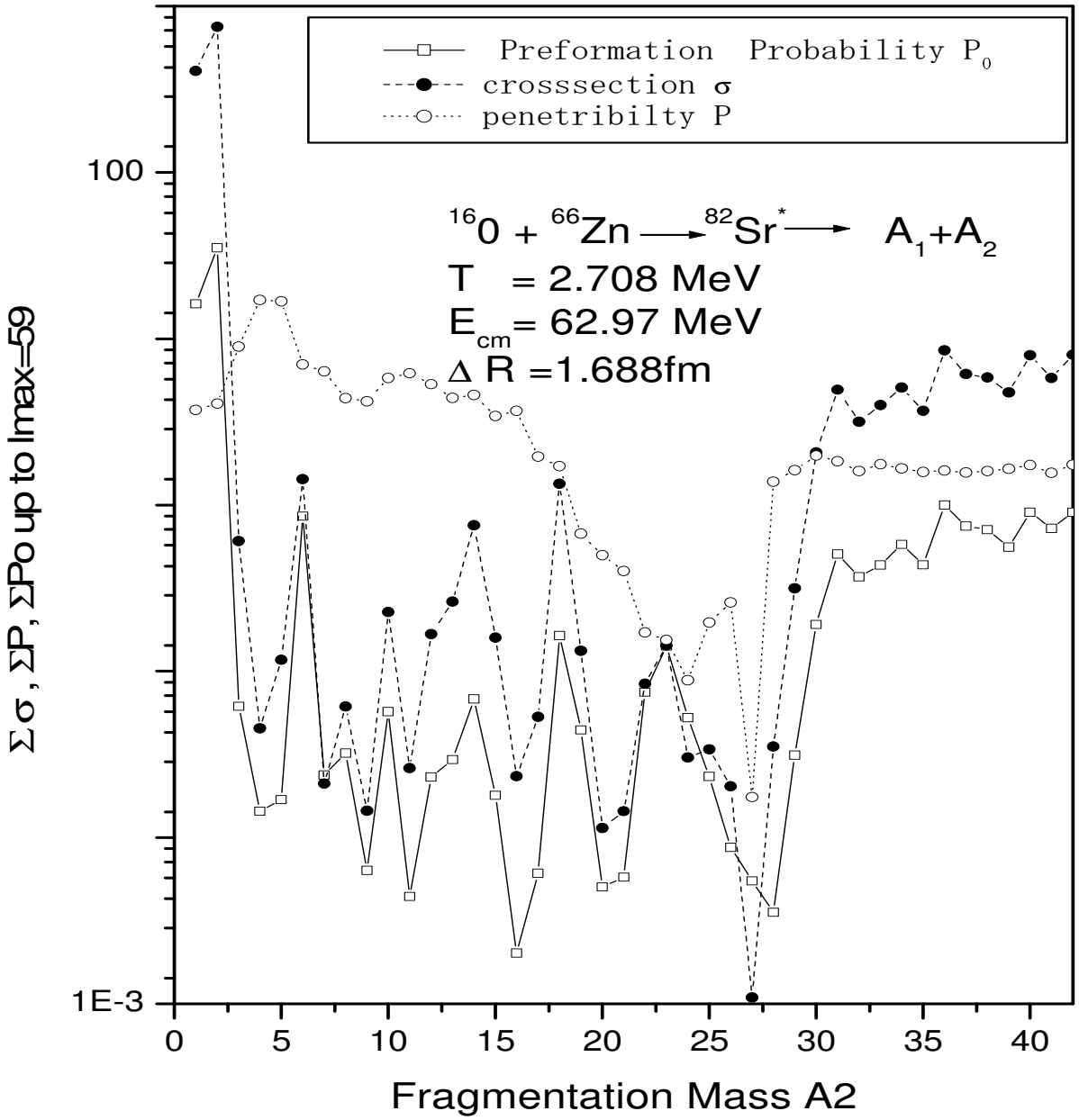

Fig. 3.4 Summed up cross section, Penetratibility, Preformation Probability as a function of fragment mass A_2 for $^{16}O+^{66}Zn\rightarrow {}^{82}Sr^{*}\rightarrow A_1+A_2$ reaction.

Fig. 3.4 shows summed up graph from ℓ =0 ħ and $\ell = \ell_{max}$= 59ħ for penetrability P, Preformation P_o and cross section as a function fragmentation mass A_2.We observe that preformation probability (open square) shows interesting structure with cross section (dark circle), On the contrary Penetrability seems to be contributing largely to magnitude and plays a silent role regarding structure expect for few fragments in intermediate mass region.

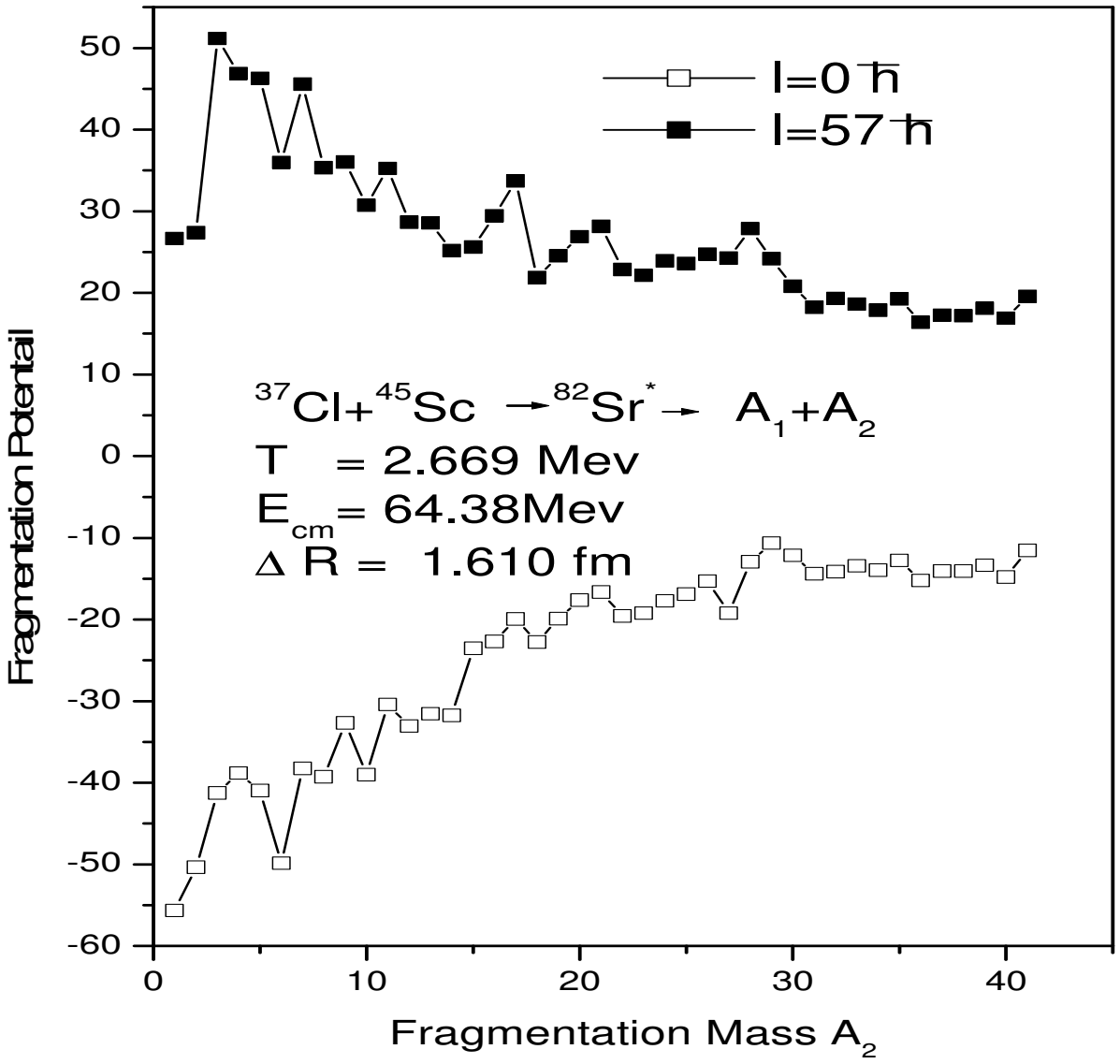

Fig 3.5 Fragmentation Potential as a function of fragment mass A_2 for $^{37}Cl+^{45}Sc \rightarrow {}^{82}Sr^{*} \rightarrow A_1+A_2$ reaction.

In fig3.5 shows the fragmentation potential as a function of fragmentation mass number $1 \leq A_2 \leq 41$ shows that at $\ell = 0\hbar$ and $\ell_{max} = 57\hbar$, $E_{c.m} = 64.38$ MeV, T=2.669 MeV, $\Delta R = 1.610$ fm for $^{37}Cl+^{45}Sc$ channel. An α- nuclear structure is obtained at both angular momentum just like $^{16}O+^{66}Zn$ channel shown in Fig 3.1with only exception that variation become relatively smooth in $^{16}O+^{66}Zn$ channel . Here also Evaporation residue is prominent at $\ell = 0\hbar$ where as at higher ℓ-values($\ell_{max}=57\hbar$) heavier mass fragments also start competing in the evaporation residue process.

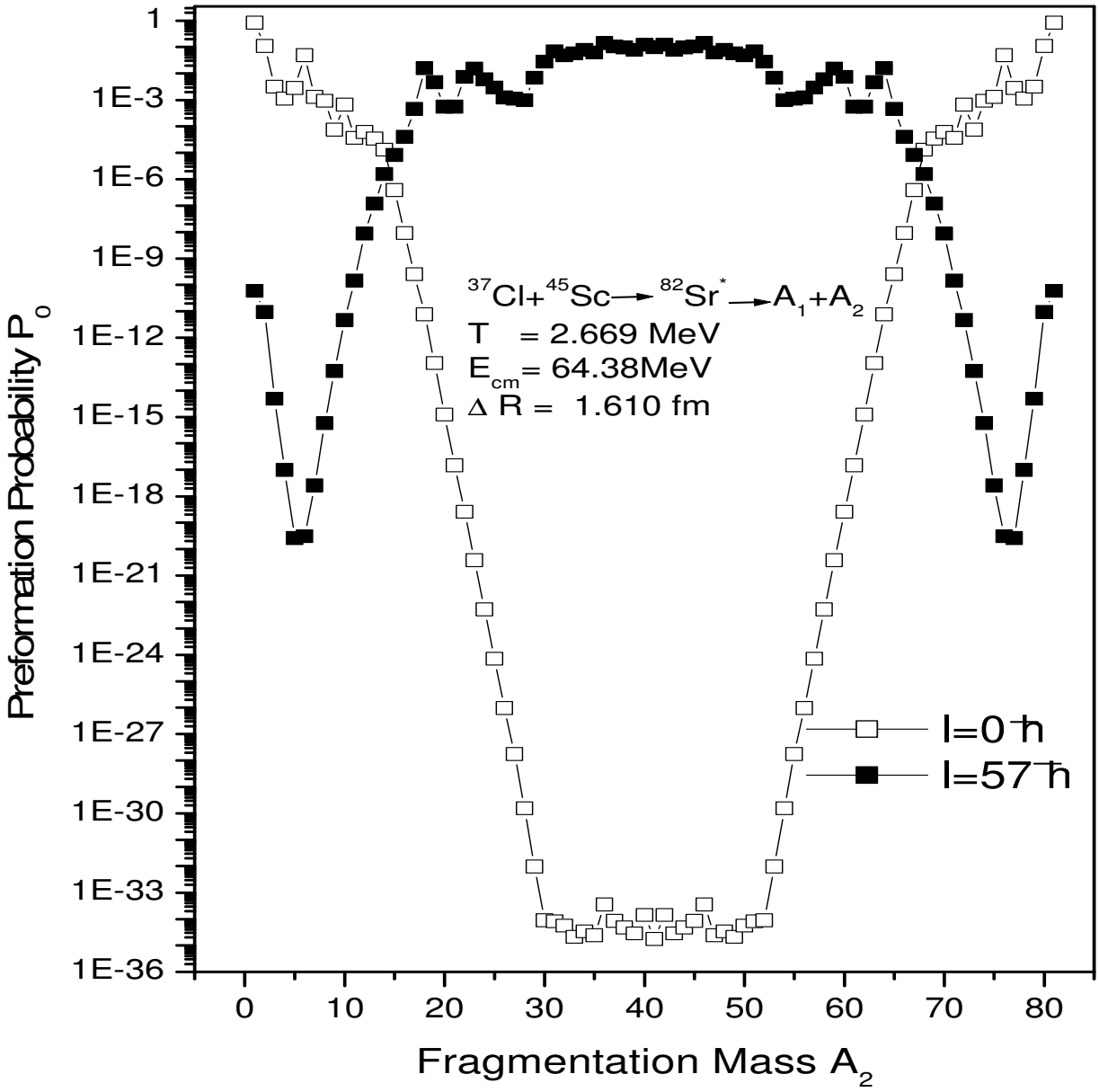

Fig.3.6 Preformation Probability as a function of fragment mass A_2 for $^{37}Cl+^{45}Sc \rightarrow ^{82}Sr^* \rightarrow A_1+A_2$ reaction.

In Fig.3.6 Preformation Probability P_0 is plotted with fragmentation mass for in $^{37}Cl+^{45}Sc$ reaction channel. Preformation Probability P_0 at ℓ = 0ħ is higher for $0 \leq A_2 \leq 4$ and then it shows a deep minima near symmetric fragments. On the contrary at ℓ_{max} = 57ħ we get enhanced probability for symmetric/near symmetric fragments as compared to light of intermediate mass fragments. It is observed clearly that variation shown in Fig.3.6 is almost similar as that for Fig.3.2

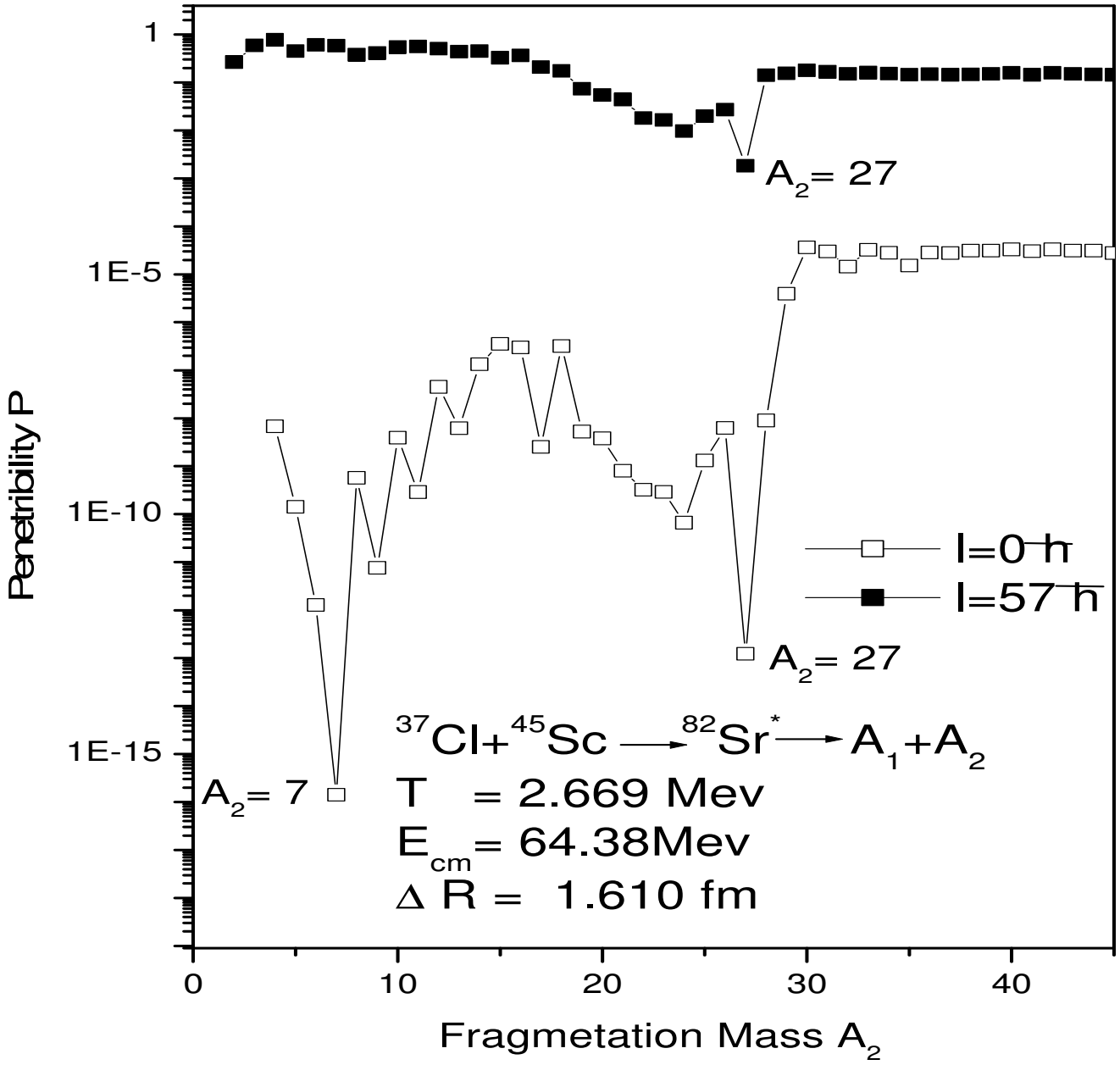

Fig. 3.7 Penetrability as a function of fragment mass A_2 for $^{37}Cl+^{45}Sc \rightarrow {}^{82}Sr^* \rightarrow A_1+A_2$ reaction.

Penetrability P measures the of capability of fragments nucleus to penetrate the potential barrier generalized during compound nucleus formation. Variation of penetration probability P with fragmentation mass A_2 is given for system$^{37}Cl+^{45}Sc$ reaction channel. The penetrability shows interesting structure for the lower ℓ &intermediate mass fragment at ℓ=0value, and become almost constant for high mass fragments. On the contrary penetrability remain almost constant for high ℓ-value, ℓ_{max}=57ħ.

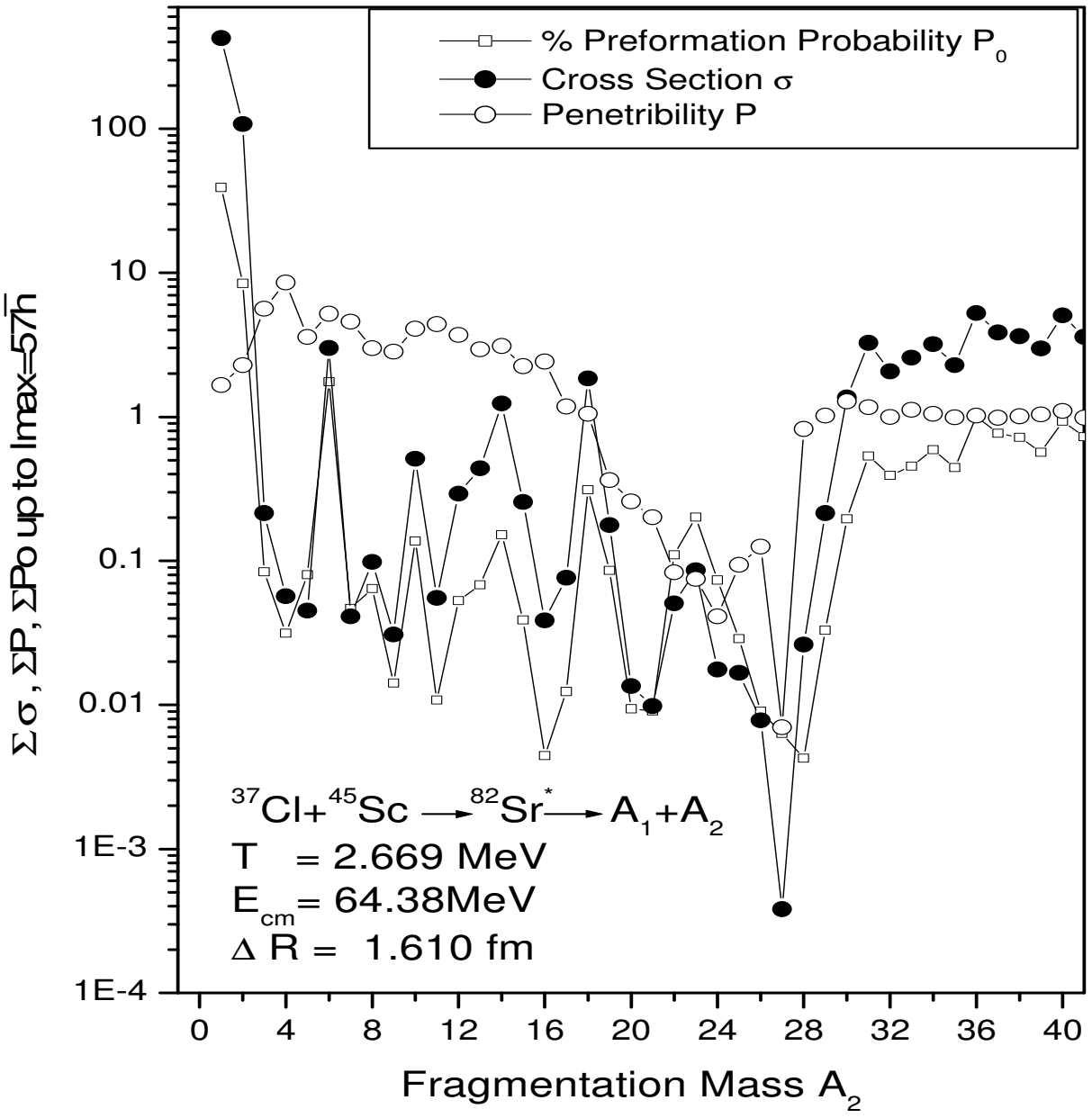

Fig 3.8 Summed up cross section, Penetratibility, Preformation Probability as a function of fragment mass A_2 for $^{37}Cl+^{45}Sc \rightarrow {}^{82}Sr^{*} \rightarrow A_1+A_2$ reaction.

Fig 3.8 shows summed up graph from $\ell = 0\ \hbar$ and $\ell = \ell_{max} = 57\hbar$ for penetrability P, Preformation P_o and cross section as a function fragmentation mass A_2. We observe that preformation probability (open square) shows interesting structure with cross section (dark circle), On the contrary Penetrability seems to be contributing largely to magnitude and plays a silent role regarding structure expect for few fragments in intermediate mass region.

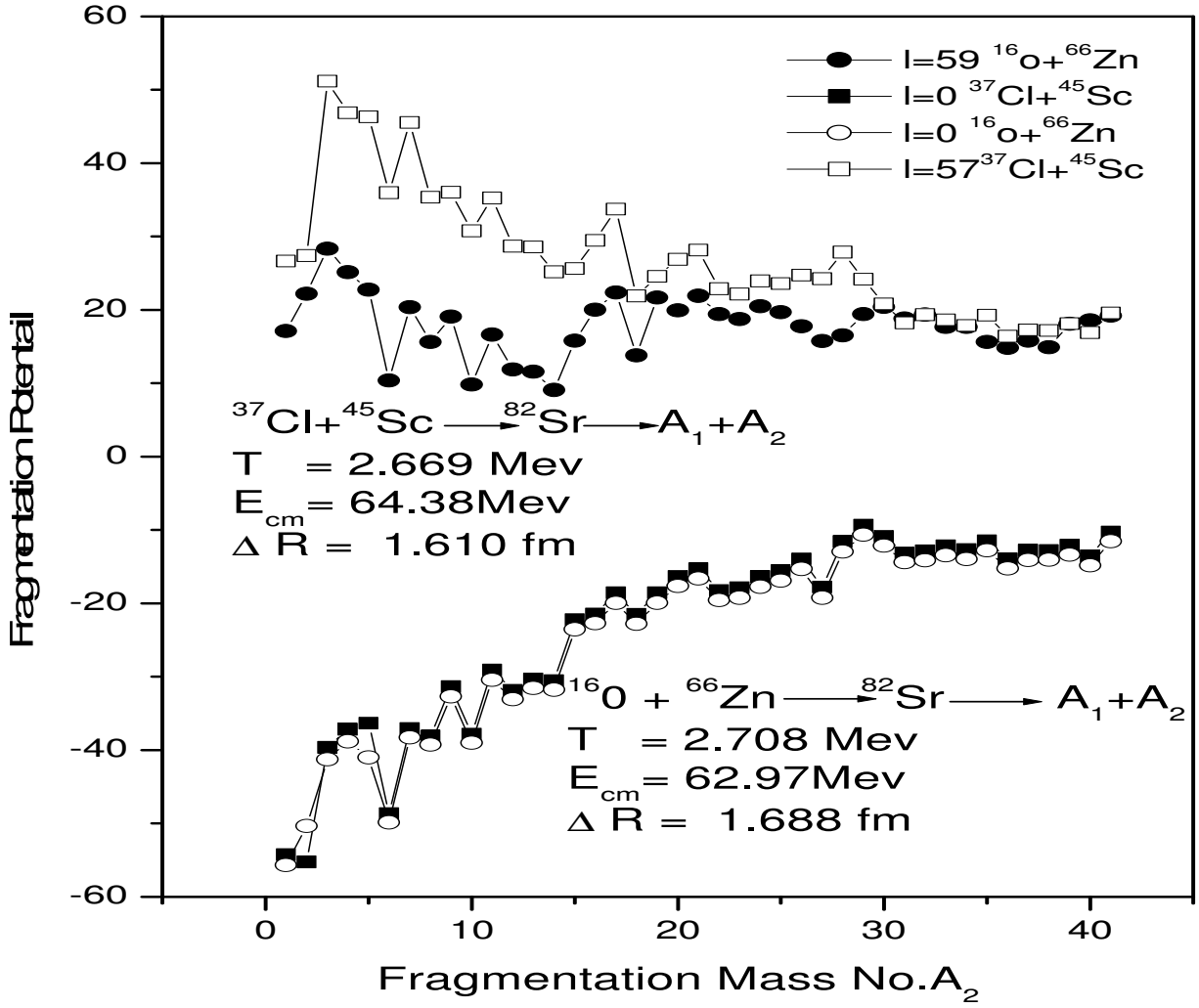

Fig.3.9 Fragmentation Potential as a function of fragment mass A_2 for $^{16}O+^{66}Zn \rightarrow {}^{82}Sr^* \rightarrow A_1+A_2$ and $^{37}Cl+^{45}Sc \rightarrow {}^{82}Sr^* \rightarrow A_1+A_2$ reactions.

Fig.3.9 shows at $\ell = 0\ \hbar$ the potential for both the reaction channels is almost identical, where as at higher ℓ-values $\ell = \ell max = 59\hbar$ for $^{16}O+^{66}Zn$ & $\ell = \ell max = 57\hbar$ for $^{37}Cl+^{45}Sc$ reaction channel. We find interesting variation in fragmentation potential especially for light and intermediate mass fragments. Two systems leading to same compound nucleus $^{82}Sr^*$shows different fragmentation potential for two different entrance channels. So fission dynamics of compound nucleus seems to be influenced by entrance channel possibly because of difference in angular momentum value $\ell = \ell max$. It is relevant to mention here that ℓmax is decided by monitoring the variation of light particles ($A_2 \leq 4$) cross section as function of angular momentum. ℓmax is chosen at the point where light particle cross section becomes negligible.

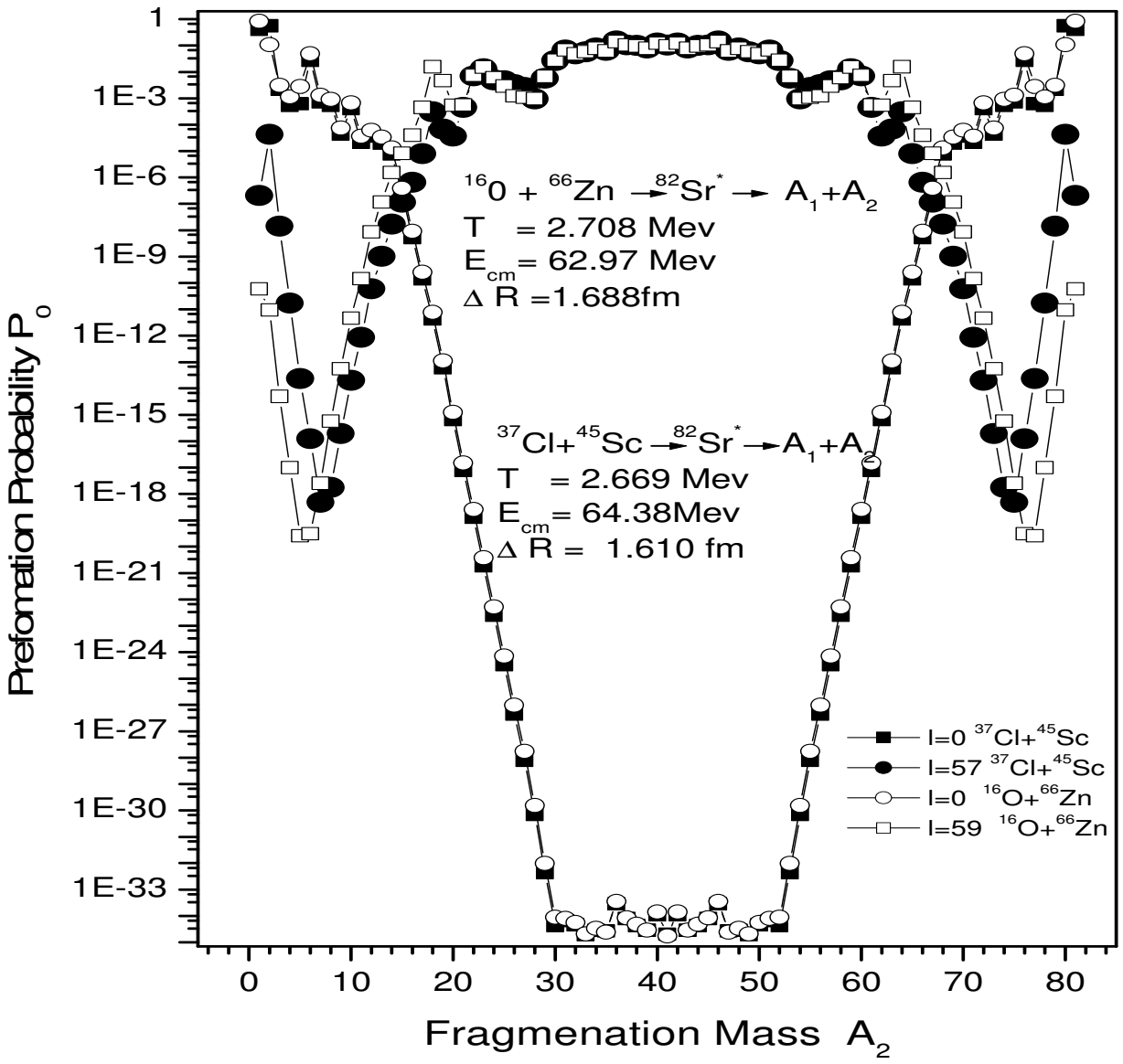

Fig.3.10 Preformation Probability as a function of fragment mass A_2 for $^{16}O+^{66}Zn \rightarrow {}^{82}Sr^* \rightarrow A_1+A_2$ and $^{37}Cl+^{45}Sc \rightarrow {}^{82}Sr^* \rightarrow A_1+A_2$ reactions.

Fig.3.10 We have plotted Preformation Probability P_o as a function of Fragmentation mass for $^{16}O+^{66}Zn$ & $^{37}Cl+^{45}Sc$ channels. The comparative behavior clearly indicate that Preformation Probability is identical at ℓ =0 ħ. However at $\ell = \ell max$ we find a significant variation in formation .Probability especially for lower& intermediate mass fragments. This result will play an important role in establishing entrance channel effect for $^{82}Sr^*$ nuclear system.

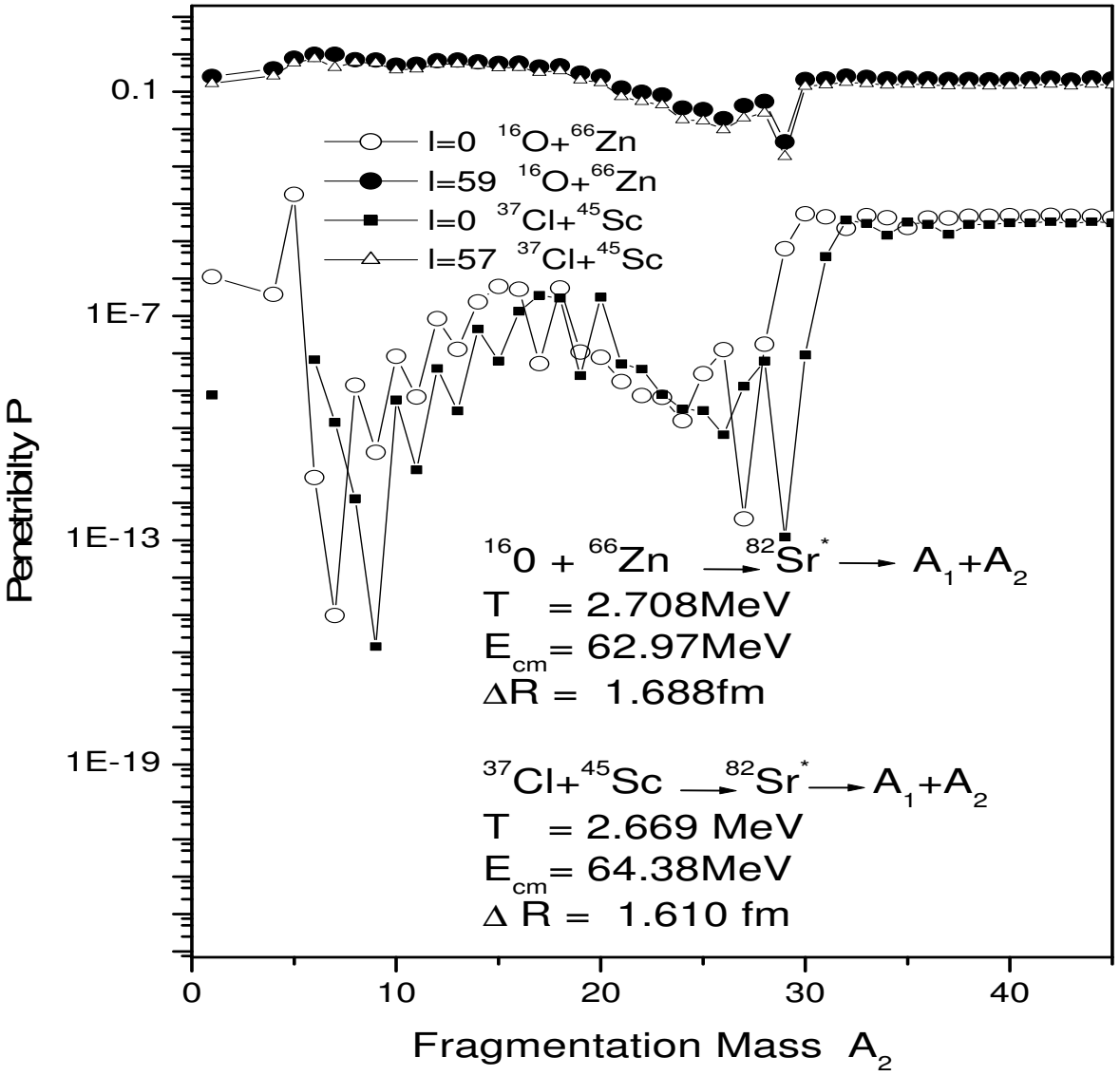

Fig.3.11 Penetrability as a function of fragment mass A_2 for $^{16}O+^{66}Zn \rightarrow ^{82}Sr^{*}\rightarrow A_1+A_2$ and $^{37}Cl+^{45}Sc \rightarrow ^{82}Sr^{*}\rightarrow A_1+A_2$ reactions.

Fig.3.11 shows that ℓ=0ħ chances of penetration are less for high mass fragments $^{16}O+^{66}Zn$ system as compared to$^{37}Cl+^{45}Sc$ system. On the contrary penetration Probability for $^{16}O+^{66}Zn$ channel shows comparative enhancement for lower and intermediate mass fragments. Interestingly at higher ℓ-values (ℓ_{max}=59ħ for$^{16}O+^{66}Zn$ & ℓ_{max}=57ħ for $^{37}Cl+^{45}Sc$ channel).There is no variation i.e both entrance channels show almost identical penetrabililty. This clearly indicate penetrability seems to be contributing in magnitude being almost structure independent.

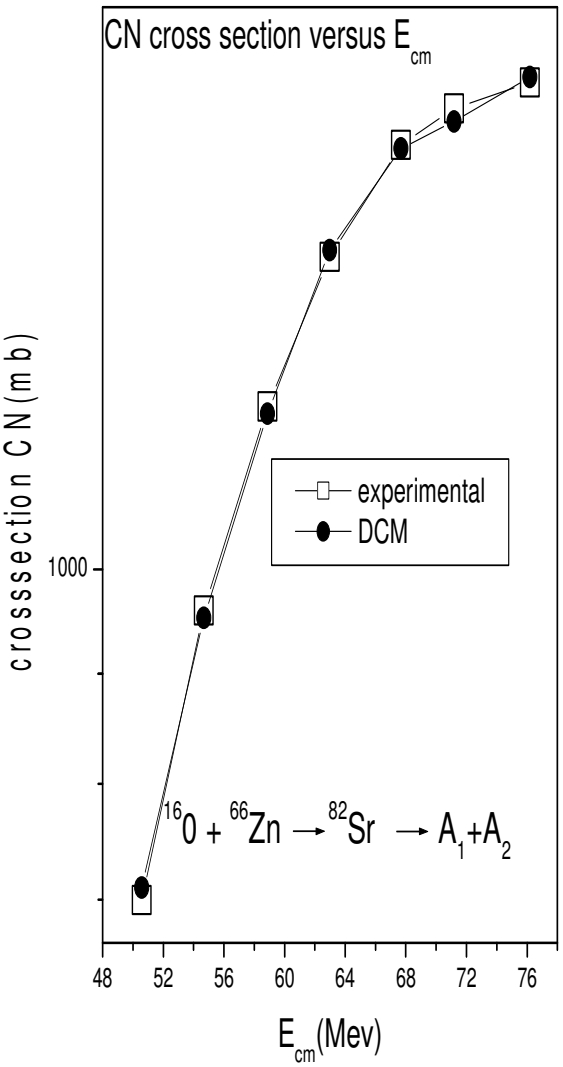

Fig.3.12(a)Comparison of DCM compound nucleus Cross section with available experiment data for $^{16}O+^{66}Zn$ reaction channel.[1]

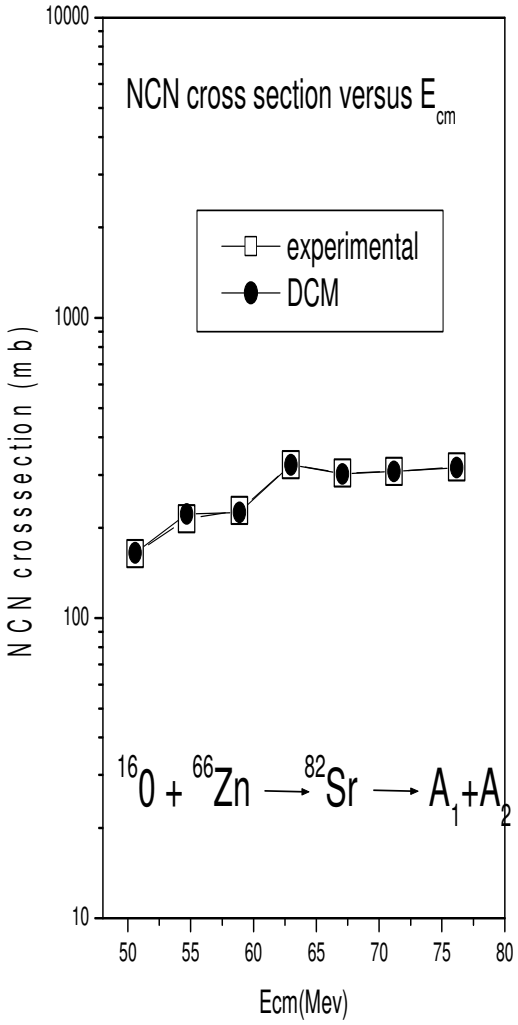

Fig.3.12(b) Comparison of DCM non compound nucleus Cross section with available experiment data for$^{16}O+^{66}Zn$ reaction channel.[1]

Fig. 3.12(a) & 3.12(b) show variation of CN cross section & NCN cross section respectively for $^{16}O+^{66}Zn$ channel. Our DCM collected cross section gives excellent agreement with experimental data at all reported excitation energy values.

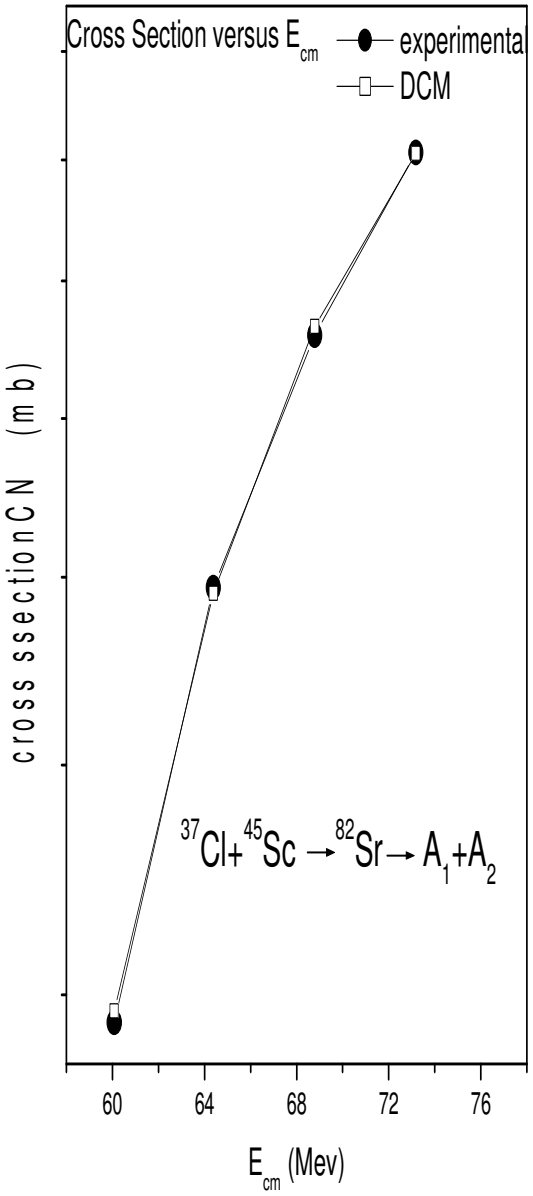

Fig.3.13(a) Comparison of DCM compound nucleus Cross section with available experiment data for $^{37}Cl+^{45}Sc$ reaction channel.[1]

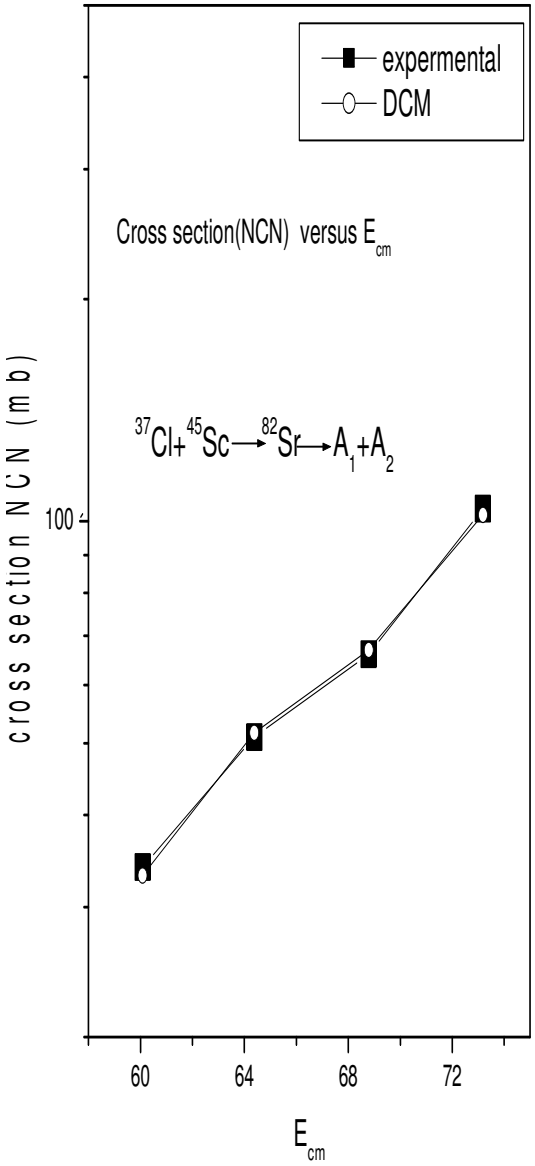

Fig.3.13(b) Comparison of DCM non compound nucleus Cross section with available experiment data for $^{37}Cl+^{45}Sc$ reaction channel.[1]

Fig.3.13(a) & 3.13(b) show variation of CN cross section & NCN cross section respectively for $^{37}Cl+^{45}Sc$ channel. Our DCM collected cross section gives excellent agreement with experimental data at all reported centre of mass energy values.

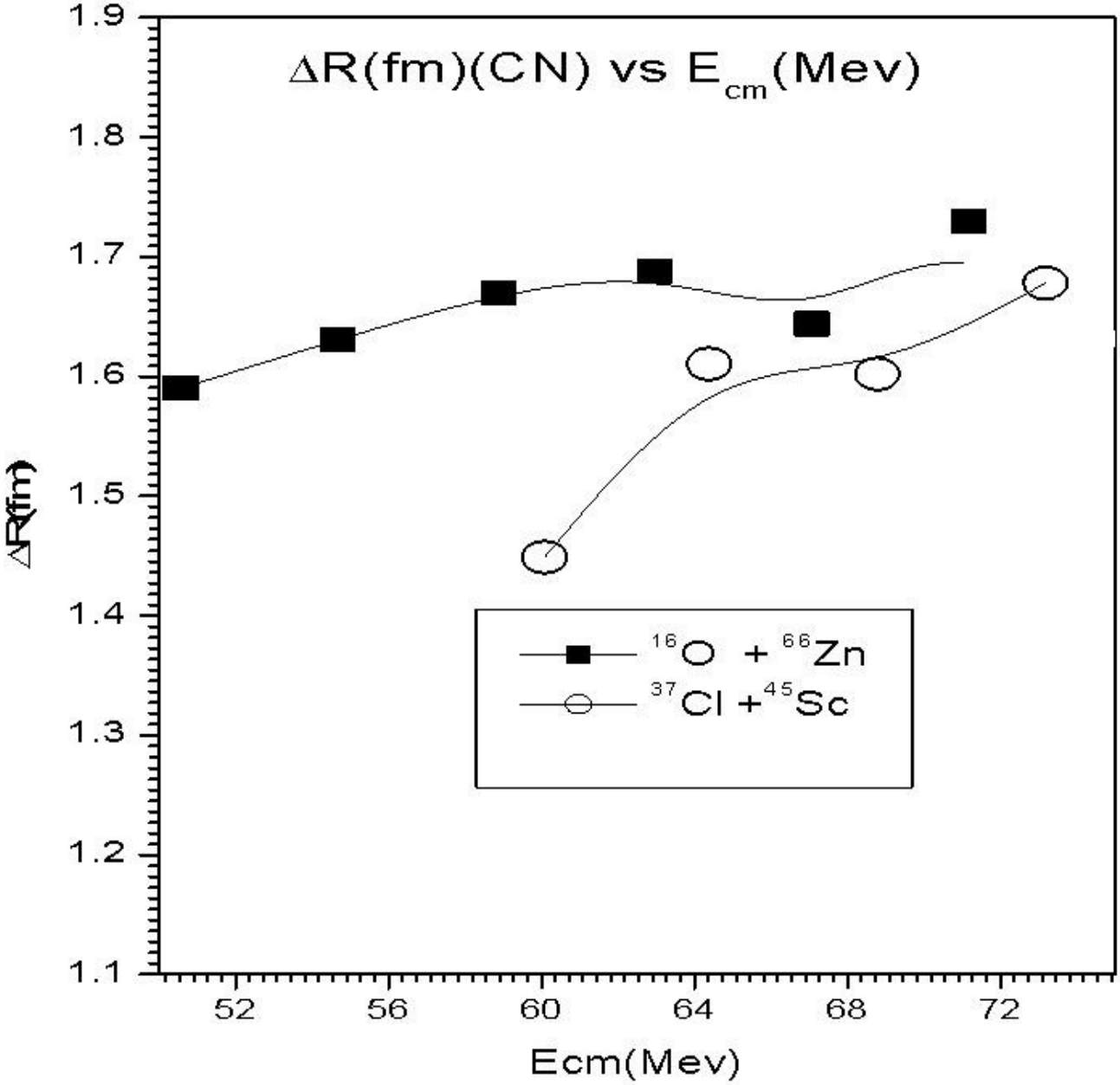

Fig.3.14 Variation of ΔR with the function of $E_{c.m}$ for $^{16}O+^{66}Zn \rightarrow {}^{82}Sr^{*} \rightarrow A_1+A_2$ and $^{37}Cl+^{45}Sc \rightarrow {}^{82}Sr^{*} \rightarrow A_1+A_2$ reactions.

Fig.3.14 gives variation of ΔR(CN) with $E_{c.m}$ for both channels. It is observed that with ΔR remain almost constant as a function of $E_{c.m}$ for $^{16}O+^{66}Zn$ channel where it increase with increase in $E_{c.m}$ for relatively symmetric channel $^{37}Cl+^{45}Sc$. It is relevant to me here that ΔR is the only parameter of model and plays an important role in deciding decay path of nuclear system formed in heavy ion reaction.

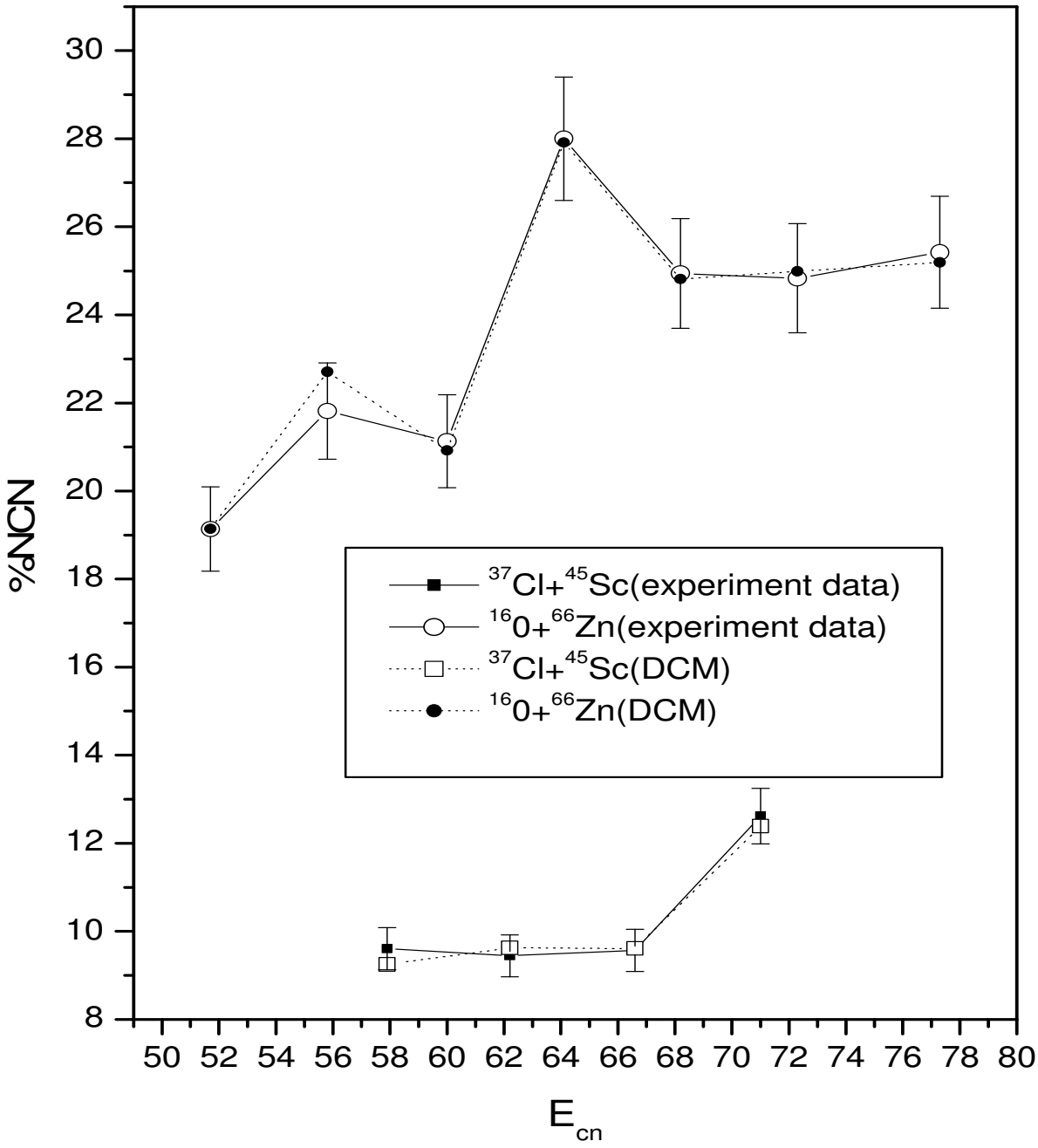

Fig 3.15 %NCN is plotted as a function of E_{cn}(excitation energy) as mentioned in Fig 4 of [1]

Calculated %NCN contribution is very much in agreement with the experimental data.

CHAPTER 4

SUMMARY AND CONCLUSIONS

Our understanding regarding formation & decay of a compound nucleus has grown significantly in view of exotic experimentation & advanced theoretical developments. Although nuclear dynamic depends heavily on temperature, energy, angular momentum, deformation etc. But another important and equivalent process is the domain of fusion fission dynamics is the concept of the entrance channel effects.

It is therefore extremely interesting & important to investigate that whether the decay path in nuclear process is entrance channel dependent or channel independent. In order to investigate such problem we have studied the entrance channel effect on the $^{82}Sr^*$ nuclear system formed by two different reactions. Our calculation clearly indicate that the fragmentation potential & preformation gets influenced by the choice of entrance channel at higher value of angular momentum ℓ_{max} which is a possible indication that decay process might be dependent on the formation channel. On the contrary penetration probability don't show such channel dependence at higher angular momentum, although a little variation is seen in the penetration path at $\ell=0$.

In this work we have studied the entrance channel effects in $^{82}Sr^*$ nucleus system formed in an asymmetric channel $^{16}O+^{66}Zn$ and symmetric channel $^{37}Cl+^{45}Sc$.Entrance channel effect in nuclear fission means decay of compound nucleus could be dependent or independent of its mode of formation. Initial state of target and projectile decide the rate of fission dynamics after the formation of compound nucleus. The Entrance Channel effects are observed to be more common for heavy nuclear system because barrier distribution angular anisotropy, mass asymmetry, deformation and orientation of nuclear systems play prominent role in the heavy mass region. But such effects are also observed in intermediate & light nuclear system.

As reported in experimental study $^{16}O+^{66}Zn$ entrance channel gives relatively more non compound nucleus cross section as compared to $^{37}Cl+^{45}Sc$,which clearly mean that $^{82}Sr^*$ seem to have entrance channel dependence .We have

carried out systematic study on the decay of $^{82}Sr^*$ formed in two extreme reaction and observe that entrance channel effect can be established using DCM calculations in agreement with experiment.

Our dynamical cluster decay model (DCM)[2-10] dependent evaporation residue and Quasi fission cross section are found to be in close agreement with experimental cross section at all reported energies. In DCM we have three important factors Preformation P_o, Penetrability P, Assault frequency ν_0. Preformation measures the probability of formation of compound nucleus when collision of target and projectile take place. Penetrability is tendency to cross the potential barrier and undergo fission. Assault frequency measures the rate of collisions undergoing with n the compound nucleus.

The only parameter of the model is neck length value ΔR, which is taken as a fitting parameter, so the variation of ΔR as a function if incident energy carries a useful information.

The variation of ΔR as a function of $E_{c.m}$ remains almost constant for $^{16}O+^{66}Zn$ where as it varies almost linearly with $E_{c.m}$ for $^{37}Cl+^{45}Sc$ channel, which again could be taken as possible indication of entrance channel dependence for $^{82}Sr^*$ nucleus.

The comparative behavior studied for $^{82}Sr^*$ nuclear system formed in two complementary entrance channel an asymmetric channel $^{16}O+^{66}Zn$ and symmetric channel $^{37}Cl + ^{45}Sc$ clearly indicate that the entrance channel does effect the decay process of this nucleus. The ℓ_{max} values (ℓ_{max} =59 ħ for $^{16}O+^{66}Zn$ & ℓ_{max} =57 ħ for $^{37}Cl+^{45}Sc$) seems to be playing important role in decay process of $^{82}Sr^*$ nuclear system. It is important to recall that the ℓ_{max} is decided on the basis of variation of evaporation residue cross section (σ_{ER}) as a function of angular momentum i.e We vary cross section as a function of angular momentum & ℓ_{max} limit when the σ_{ER} become zero or negligibly small.

REFERENCE:

[1] SUPARNA SODAYE, B S TOMAR and A GOSWAMI
Radiochemistry Division, Bhabha Atomic Research Centre, Mumbai 400085, India Corresponding author. MS received 27 December 2005; revised 15 February 2006; accepted 15 April 2006
Vol. 66, No. 6 | journal of June 2006

[2] R.K. Gupta, M. Balasubraniam, C. Mazzocchi, M. La Commara, and W. Scheid, Phys. Rev. C 65, 024601 (2002).

[3] M.K. Sharma, R.K. Gupta, and W. Scheid, J. Phys. G 26, L45 (2000).

[4] R.K. Gupta, R. Kumar, N.K. Dhiman, M. Balasubraniam, W. Scheid, and C. Beck, Phys. Rev. C 68, 014610 (2003).

[5] R.K. Gupta, W. Scheid and W. Greiner, Phys. Rev. Lett. 35, 353 (1975).

[6] R. K. Gupta, IANCAS Bull. (India), 6, 2(1990).

[7] R.K. Gupta, N.Singh, and M. Manhas, Phys. Rev. C 70, 034608 (2004)

[8] R.K. Gupta ,M.balasubramaniam, R.Kumar, N.Singh, M.Manhas, and W. Greiner, J.Phjs. G: Nucl.Part. Phys. C 31, 631(2005).

[9] S.S. Malik and R.K.Gupta, Phys.Rev.C 39, 1992(1989)

[10] R.K.Gupta, W.Scheid, and W.Greiner, J.Phys.G:Nucl. Part. Phys. 17, 1731(1991).